
University of South Australia

The Library
www.library.unisa.edu.au

Educating Professionals, Creating and Applying Knowledge, Engaging our Communities

NOTICE: this is the accepted author manuscript (AAM) or post-print which was accepted for publication in **'Environmental Modelling and Software'**. Changes resulting from the publishing process, such as peer review, editing, corrections, structural formatting, and other quality control mechanisms are reflected in this document. A definitive version was subsequently published in **'Environmental Modelling and Software', vol. 79, pp. 167-183, 2014. DOI:** 10.1016/j.envsoft.2016.02.006

Quantifying the impacts of artificial flooding as a salt interception measure on a river-floodplain interaction in a semi-arid saline floodplain

S. Alaghmand (corresponding author) [1, 2], S. Beecham[2], J.A. Woods[3, 4], K.L. Holland[4], I.D. Jolly[4], A. Hassanli [2,5] and H. Nouri [2]

[1] Discipline of Civil Engineering, School of Engineering, Monash University (Malaysia Campus), Malaysia

Email: sina.alaghmand@monash.edu

[2] Centre for Water Management and Reuse (CWMR), School Natural and Built Environments (NBE), University of South Australia, Australia

[3] National Centre for Groundwater Research and Training, Flinders University, Bedford Park, Australia

[4] Commonwealth Science and Industrial Research Organisation Land and Water Division, Glen Osmond, Australia

[5] College of Agriculture, Shiraz University, Iran and Adjunct Associate Professor, CWMR, School of NBE, University of South Australia

Highlights

- We quantified impacts of artificial flooding on saline floodplain and its ecological implications.
- Combination of artificial flooding and groundwater lowering resulted in a 4% decrease in solute mass.
- Groundwater discharges to the river following artificial flooding cannot increase river salinity.
- Artificial flooding can temporarily form less saline groundwater and soil profiles that improve water availability for vegetation.
- Artificial flooding may be considered as a short term management technique and needs to be applied periodically.

Abstract

The natural flow regime of the Lower Murray River in South Australia has been altered and resulted in severe decline in the condition of long-lived vegetation on the floodplain. This paper aims to quantify the relative impacts of artificial flooding on the flow and solute dynamics of the floodplain aquifer and its ecological implications. It is shown that artificial flooding can temporarily form less

saline groundwater and soil profiles which in turn improves water availability for vegetation. From ecological point of view, artificial flooding delivers some of the same benefits as natural overbank floods. However, the washed-off solute mass from the soil profile was only sustained for 4 to 6 months. It appears that artificial flooding is an intervention technique that is limited spatially to the flooded area and temporally to the flood duration. Hence, it may be considered as a short term management technique in arid and semi-arid areas.

Keywords: Artificial flooding, surface water and groundwater interaction, semi-arid floodplain, unsaturated zone stored solute, HydroGeoSphere, Lower Murray River.

Software:

Name of software: HydroGeoSphere

Developers: R. Therrien (Universite Laval), R.G. McLaren, E.A. Sudicky, Y-J. Park (University of Waterloo)

Contact address: 564 Weber Street North, Unit 12, Waterloo, ON, N2L 5C6 (http://www.aquanty.com)

Telephone: (519) 279-1080

Fax: (519) 279-1081

E-mail: sales@aquanty.com

Hardware required: Any Microsoft Windows based PC with sufficient RAM

Software required: FORTRAN 95 (The software is compatible with postprocessors such as ParaView, GMS, Tecplot and etc.)

1 Introduction

Nearly all rivers in the world are to some extent influenced by human activities. River systems usually include floodplains and therefore an important component of the system is the interaction of surface water (SW) and groundwater (GW). From a salinity perspective, floodplains often play a significant role. In many cases, particularly in arid and semi-arid areas, floodplain aquifers may act as a source of solute or as a pathway for solute mobilization towards the river (Alaghmand et al., 2013a). It is well-understood that there is a dynamic interaction between these two domains hydraulically, ecologically and hydrologically (Karim et al., 2012; Motta et al., 2012; Russo et al., 2012; Zilli and Paggi, 2013). Moreover, human agricultural activities on the floodplain and adjacent highland, such as excess drainage and groundwater extraction, may cause soil salinity issues, increased groundwater levels and groundwater quality declines that can influence the river flow quality and quantity (Brunner et al., 2007; Brunner et al., 2008; Nouri et al., 2013). However, many of these activities are unavoidable due to human population growth and the limited nature of available natural resources. The Lower Murray River is a typical example of a semi-arid area where changes to floodplain hydrology have caused a decline in the condition of the dominant riparian tree species (*Eucalyptus largiflorens,* black box; *E. camaldulensis,* river red gum; and *Acacia stenophylla,* river cooba) due to groundwater and soil salinization (Maheshwari et al., 1995; Slavich et al., 1999). More than 75% of all trees along the Lower

Murray River floodplain in South Australia were classified as unhealthy in 2002-2003 (Smith and Kenny, 2005). Overbank flooding is a key hydrologic process affecting floodplain aquifer flow and solute dynamics and ecological processes such as biogeochemical cycling and plant diversity (Doble et al., 2012; Naiman and Décamps, 1997). Overbank flooding historically occurred for a few days to weeks every few years for most natural rivers (Wolman and Leopold, 1957). But in the Lower Murray River a system of major reservoirs and small locks and weirs were installed along the river during the 1920s to regulate river flow and provide a navigable passage. This led to the raising of groundwater levels beneath the adjacent floodplains together with a reduction of frequency of medium to large floods by a factor of three (Alaghmand et al., 2014a; Ohlmeyer, 1991). This was combined with an absence of overbank flooding between 1994 and 2010 during the "Millennium Drought" (Leblanc et al., 2012; Timbal et al., 2010). One of the consequences was an increase in soil and groundwater salinity in the floodplains that has reduced water availability for riparian vegetation due to increased osmotic potentials (Busch and Smith, 1995; Jolly et al., 1993; Munns, 1993). Figure 1 shows the conceptual model of the river-floodplain system influenced by human-induced activities at the Lower Murray River.

Numerical models are one of the most popular tools that can be used to explore the relative importance of each SW-GW interaction process (Rassam et al., 2013; Sophocleous, 2002). For many years in modelling practice, the surface and subsurface domains were considered separately which is not a realistic assumption particularly in areas with dynamic and hydraulically well-connected SW and GW systems (Furman, 2008). In fact, physically based numerical modelling has an established role in water resources management, but such models conventionally treat GW and SW as independent parts of the hydrological system. This inherent deficiency was first recognised in the late 1960s by Freeze and Harlan (1969). Recent advances in the numerical modelling have led to fully integrated modelling tools that allow solving both the surface (lakes, streams and wetlands) and sub-surface (unsaturated and saturated GW flow) domains simultaneously using a single matrix of equations (Ala-aho et al., 2015). The development of fully integrated models have provided the conventional saturated groundwater flow equation with the capability to account for variably saturated flow using a modified form of the Richards equation (Richards, 1931). These type of models have been used to simulate SW-GW interactions at various scales (Alaghmand et al., 2014b; Brookfield et al., 2009; Li et al., 2009; Smerdon et al., 2007; Smith et al., 2008; Sudicky et al., 2008; Trigg et al., 2014). Alaghmand et al. (2013b) concluded that a 3D fully-integrated physically-based surface-subsurface numerical model with the capabilities of saturated-unsaturated modelling and solute transport simulation is required for detailed modelling of river and floodplain interactions. However, high quality observed data are also an essential part of these studies to establish a reliable, validated model. In fact, fully integrated models, like spatially distributed model in general, have difficulties in estimating representative parameter values and boundary conditions needed to solve the governing flow equations (Ala-aho et al., 2015; Beven, 2002).

Zimmermann et al. (2006) studied salt transport on islands in the Okavango Delta using SEAWAT code (Guo and Langevin, 2002), which is in fact the combination of MOD-FLOW (Harbaugh and M.G., 1996) and MT3DMS (Zheng and Wang, 1999). They used geophysical observations to calibrate the model and demonstrated the density fingering processes. They concluded that the results were sensitive to changes of the hydraulic gradient and the evapotranspiration rate, as small changes may lead to different plume developments. Bauer et al. (2006) conducted another study at the Okavango Delta to gain further understanding of the complex interactions of different processes that led to the

present state of the study site (Shashe River Valley) and to predicting the future development under different scenarios. The study showed that in semi-arid and arid regions a coupled approach to flow and transport modelling is essential. Also, they concluded that evaporation and transpiration are key processes in such systems. In this context, remote sensing (RS) data contain information that can help in setting up and verifying a groundwater model. For instance, ET can be calculated from RS images based on the theory of surface energy balance (Roerink et al., 2000). Then, a comparison between the ET from RS data, groundwater model and field data can be carried out (Kite and Droogers, 2000). Brunner et al. (2007) and Brunner et al. (2008) used remote sensing spatial distributed data to develop phreatic evaporation and soil salinization risk, respectively, in the Yanqi basin located in western China. Later, Li et al. (2009) used the same approach to investigate different groundwater abstraction schemes on solute dynamics and surface water conditions. They used the spatial distribution pattern of evaporation data from the RS images in the model calibration process. They showed that use of evaporation pattern information obtained from RS can reduce the limitations of a small number of hydraulic head data available for groundwater model calibration. Furthermore, Geng and Boufadel (2015) conducted a numerical study, using a density-dependent variably saturated groundwater flow model MARUN, to investigate subsurface flow and salt transport in bare saline aquifers subjected to high rate of evaporation.

The main objective of this paper is to integrate field data in a complex model towards better understanding of new salinity management options. To do this, firstly, the interaction between a river and a semi-arid saline floodplain is modelled based on observed data at a study site, where it is significantly influenced by artificial flooding and groundwater lowering. Then number of scenarios are conducted to quantify the individual impacts of each driver using a fully-integrated physically-based flow and solute numerical modelling approach. The research question is what are the impacts of artificial flooding and groundwater lowering on the floodplain aquifer flow and solute dynamics and what are the ecological implications. The impacts are discussed in terms of water and solute balances. Also, the ecological implications of artificial flooding are examined to see if vegetation health condition improves and is sustained after the flooding events.

2 Methods

The numerical model employed here is based on a conceptual model of a river and a saline floodplain system at Clark's Floodplain located on the Lower Murray River in South Australia. Prior to European settlement there was a natural balance between the river and the saline regional groundwater. But after river flow manipulation by installation of weirs along the river, and irrigation practices in the adjacent highlands, the water table level in the floodplain has been increased. The raised groundwater level beneath the floodplain has led to increased rates of groundwater evapotranspiration. Because the groundwater is naturally saline, the increased ET results in floodplain salinization, which consequently affects the health of floodplain vegetation (Alaghmand et al., 2014a). Therefore, artificial flooding has been examined as a salt management measure to mobilize some of the accumulated solute from the unsaturated zone and to increase water availability for the stressed vegetation.

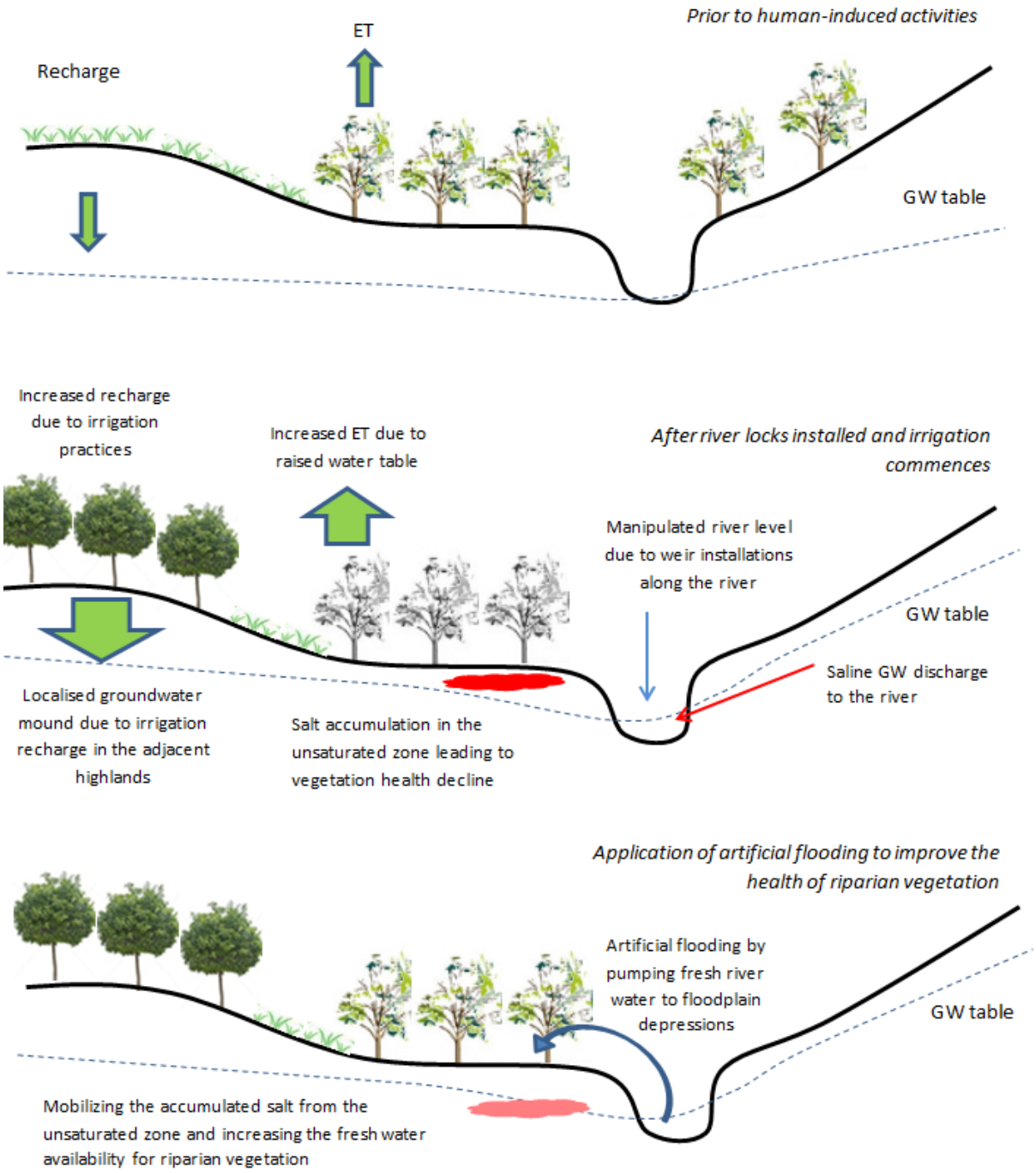
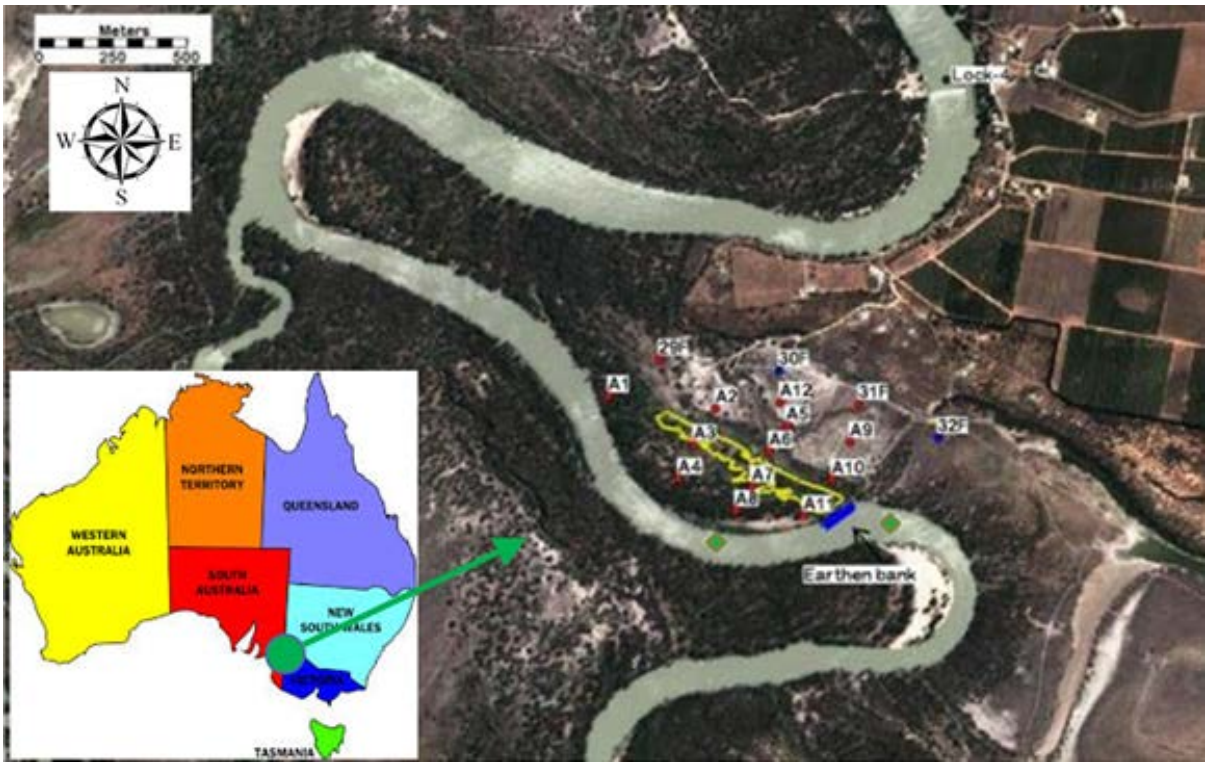


Figure 1. Conceptual model of the river-floodplain system influenced by human-induced activities (Adopted from Alaghmand et al. (2014a))

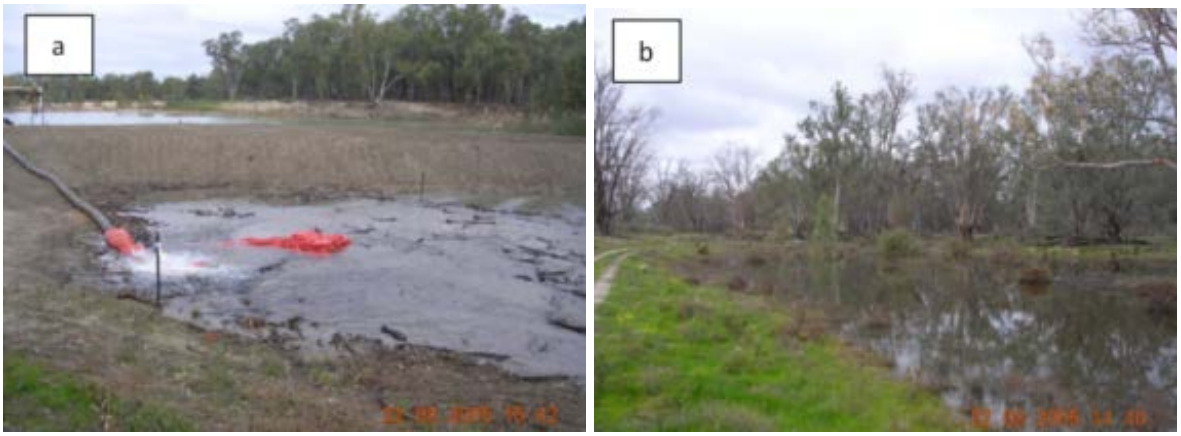
2.1. Study Site

Clark's Floodplain is located on the Lower Murray River in South Australia (34°21'S, 140°34'E), downstream of Lock and Weir No. 4 (Figure 2a). The climate in the Lower Murray River is semi-arid with mild winters and long hot summers. Annual potential pan evaporation (1900 – 2000 mm) is over seven times the average annual rainfall (250-260 mm) (BOM, 2013). The floodplain is located next to the Bookpurnong Irrigation District which was developed in 1964. Irrigation has created a localised groundwater mound in the regional Loxton-Parilla Sands aquifer, increasing the hydraulic gradient towards the floodplain and causing an increase in groundwater flux to the river and seepage of saline

groundwater at the edge of the river valley (Holland et al., 2013). In order to maintain the River Murray water quality, a series of production wells along the floodplain were constructed in 2005. These wells are known as the Bookpurnong floodplain salt interception scheme (SIS) which aims to reduce the hydraulic gradient that drives the regional saline groundwater towards the River Murray by maintaining the watertable between the SIS bores at river level. The SIS bores (30F and 32F) were operational between August 2005 and November 2006 and between May 2007 and a flood that occurred in 2010/11 (White et al., 2009). Two of the SIS production wells are located in the study site, namely 30F and 32F, which are shown in Figure 2a.



a.



b.

Figure 2. a: Configuration of the study site. Observation wells and SIS production wells are shown in red and blue circles, respectively. The yellow line indicates the floodplain depression. The green diamonds represent river salinity loggers. Inset map shows the location of the study site in Australia.

b: Clark's Floodplain depression during the second trial in August 2005 (a: River Murray water is pumped to the depression over the constructed earthen bank, b. the floodplain depression is filled with the river water) (White et al., 2009)

The Lower Murray River floodplain in South Australia is typically vegetated by a mixture of *Eucalyptus camaldulensis* (red gum), *Eucalytpus largiflorens* (black box), *Acacia stenophylla* and *Muehlenbeckia florulenta* (lignum) (O'Malley and Sheldon, 1990). The existence of river red gums shows that the floodplain depression was naturally flooded every 3 to 5 years before regulated flow regimes were instituted (White et al., 2009). Soils in the study area generally consist of micaceous cracking clay deposits, known as the Coonambidgal Clay which overlies the Monoman Formation, an aquifer unit composed of unconsolidated sand deposits with variable clay and silt content that is hydraulically connected to surface water bodies on the floodplain (Jarwal, 1996). Within the River Murray valley, the Monoman Formation aquifer is in direct contact with the regional Loxton-Parilla Sands. Groundwater salinities in the study area can be divided into two zones, namely a relatively fresh water zone (<5,000 µS/cm) in parts of the floodplain aquifer nearest to the river and another zone where salinity levels are in excess of sea water (up to 50,000 µS/cm) in areas away from the river bank (White et al., 2009). In fact, the regional aquifer acts as the main source of solute flowing towards the floodplain and eventually the river.

A total of 12 observation wells were constructed at the study site in June 2005 to record the groundwater level and salinity using pumping/bailing methods (Figure 2a). Also, soil samples were collected in 0.5 m increments from the unsaturated zone during installation of the twelve wells on a bi-annual cycle until March 2008. Furthermore, a Geonics EM31 conductivity meter survey was conducted at the study site on six occasions; June 2005, February 2006, September 2006, February 2007, September 2007 and March 2008 (White et al., 2009). Moreover, recorded meteorological data such as rainfall and potential evaporation were obtained from the Loxton Research Centre meteorological station (ID: 024024) (BOM, 2013). The Murray River recorded flows were obtained from the water level station downstream of Lock 4, which is situated immediately upstream of Clark's Floodplain (ID: A4260515) (WaterConnect, 2013). Likewise, River salinity observations were obtained from the Clarke's Sandbar (ID: A4261066) and Rilli Island (ID: A4260642) stations located upstream and downstream of the study site, respectively (Figure 2a).

This paper focuses on two rounds of artificial flooding (hereafter referred to as *trials*) that were conducted by White et al. (2009) at a depression located at the northern end of Clark's Floodplain near the river. Hence, all the field data were obtained from White et al. (2009) in order to build the study site model. An 80 m earthen bank was constructed at the southern end of the floodplain depression where a flood-runner normally fills it from the river (Figure 2b). The construction of the earthworks formed an inundation zone that covered 3.7 ha of the depression with a 10.7 ML capacity. Fresh water from the river was pumped over the earthen bank in the depression. Two artificial floods (29.97 ML between 25 July and 30 August 2005 and 52.17 ML between 25 September and 5 December 2006) kept the water level to the 12.0 m AHD (Australian Height Datum) contour, holding the water at 1 m depth in the deepest point throughout the duration of the trials. In addition, two of the SIS production wells were located in the study site and were in operation during the study period except from November 2006 to May 2007. During this period the wells were shut down due to technical problems. When they were in operation they were extracting the groundwater at a rate of 1-3 L/s. The groundwater lowering began operation mid-way through the first inundation and stopped mid-

way during the second inundation due to a fault in the disposal pipeline. These irregularities in SIS operation affected groundwater levels, which accompanied with river levels rise caused difficulties in interpreting groundwater levels and salinity data due to each of the events. After the second trial of artificial flooding, when no water was pumped to the floodplain depression, a decrease in water levels across all wells was recorded, correlating with the decrease in river levels.

2.2. Numerical Model Set-up

2.2.1 HydroGeoSphere

The HydroGeoSphere (HGS) model (Therrien et al., 2006) was selected for this study because of the hydrological processes involved, including bank recharge, surface recharge (artificial flooding, rainfall), possible river depletion, groundwater lowering and evapotranspiration (ET). Moreover, HGS was chosen over more commonly used numerical models such as MODFLOW. Brunner 2010 et al. (2010) showed that HGS is a more sophisticated model that includes a more realistic physical coupling between surface water and groundwater. This is particularly the case when considering the unsaturated zone, for accurate estimation of infiltration rates under a river and for inclusion of a transition zone (Brunner et al., 2010). Further details on the code and a recent review of software are provided by Therrien et al., (2006) and Brunner and Simmons (2012), respectively. Here, HGS used the control volume finite element method to solve the flow equations for all domains considered in the simulation, and the control volume finite element method to solve the transport equation. A dual node approach was used to couple the surface and sub-surface domains (Liggett et al., 2012). The model solves non-linear equations for variably-saturated subsurface flow, surface flow and solute transport. For further details on the model and governing equations, the reader is referred to Therrien et al. (2010).

2.2.2 Model domain and grid

HGS is a fully-integrated surface-subsurface numerical model. In this context, parameter values for the subsurface domain (porous media) and surface domain (river and floodplain) and ET are assigned separately. Hence, the river-floodplain system was conceptualized as a zone of porous media (consisting of the three soil formations), overlain by surface flow cells (consisting of the river, the floodplain (and the highland)). The surface flow cells allow the river to flow up its banks, so that the river width increases during high flows. The domains were linked with a dual node arrangement, with a coupling length of 0.01m. Previous research has showed little sensitivity to coupling length for values less than this (Doble et al., 2012).

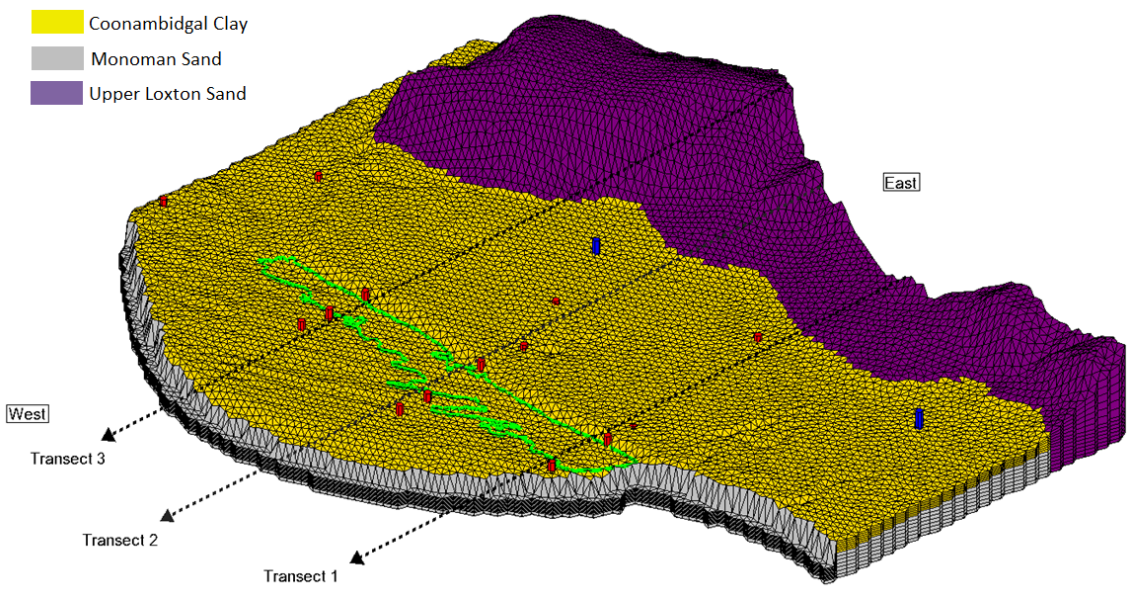
As illustrated in Figure 3a, the geometry grid covered 92 ha of Clark's Floodplain and a 1,550 m length of the river bank. According to the available drill log data (DES, 2013) three soil types were included in the model, namely Coonambidgal Clay, Monoman Sand and Upper Loxton Sand. The geometry grid of the study site was built using available GIS and LiDAR data. For this study, a digital elevation model of the study site was generated at a 10 m grid resolution using LiDAR data. A total of 15 non-uniform sub-layers were built ranging from 0.1 m up to 2.0 m in thickness including finer grids in the upper layers to model more efficiently the flow and solute exchange processes occurring between the surface and sub-surface domains. The final grid geometry consisted of 146,800 nodes that formed 269,925 elements. Figure 3b shows the model domain and the geometry grid of the study site.

2.2.3 Domain properties

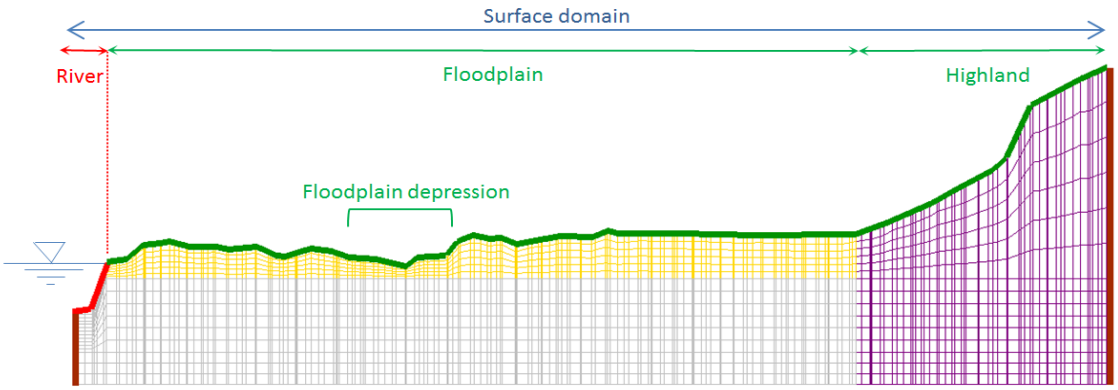
The properties of the subsurface domain (porous media) of the model and unsaturated van Genuchten function parameters (van Genuchten, 1980) were adopted from Jolly et al. (1993) and Doble et al. (2006) who adjusted and proposed van Genuchten parameters for the Lower Murray River soil types including semi-confining heavy Coonambidgal Clay, Monoman Sands and Upper Loxton Sands.

An ET function was applied to the surface domain. Two different ET function parameter values were considered according to the vegetation cover of the study site. As shown in Figure 3c, the study site is covered by Eucalyptus trees and grass. The ET parameter values for Eucalyptus and grass were adopted from Doody et al. (2009), Banks et al. (2011) and Verstrepen (2011).

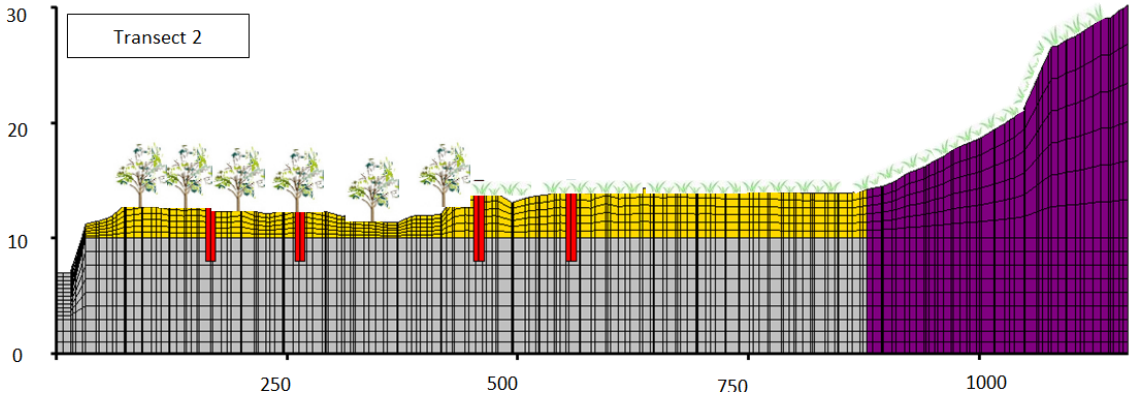
Under natural conditions, surface hydraulic parameters such as friction (x and y-planes), rill and obstruction storage height and coupling length have significant differences. So, the surface domain was divided into the main channel (the river) and the floodplain (including the highland). Moreover, riverbed hydraulic conductivity can vary spatially and temporally over several orders of magnitude (Calver, 2001; Wang et al., 2014). This can be due to erosion/deposition events (Hatch et al., 2010), biological activities (Treese et al., 2009) and temperature dependent material properties (Engeler et al., 2011). However, in numerical modelling studies the riverbed is often conceptualized as a homogeneous geologic structure with properties obtained through model calibration because quantifying riverbed heterogeneity in the field is often challenging. So, the riverbed complexity is replaced with homogeneous equivalents. Irvine et al. (2012) showed that understanding the state of connection is the key to quantifying potential errors produced by numerical models when homogeneous equivalents are obtained by means of model calibration. They concluded that in connected and disconnected flow regimes, as defined by Brunner et al. (2009a) and Brunner et al. (2009b), homogeneous equivalence is an efficient assumption. However, in a transitional regime a homogeneous equivalent will result in errors for simulations of both a rising and falling water table (Irvine et al., 2012). In this case, the river-floodplain is a connected flow regime during the study period. The surface flow domain properties were adopted from Doble et al. (2012), Banks et al. (2011), McCallum et al. (2010). All the model parameters values are summarized in Table 1.



a.



b.



c.

Figure 3. a: 3D illustration of the study site (Z magnification: 5). Observation wells and SIS production wells are shown in red and blue circles, respectively. The green line indicates the extent of the floodplain depression. b: Conceptual configuration of the surface domain including the river (shown in red), the floodplain and the highland (shown in green). c: Soil layers and conceptual vegetation cover along Transect 2.

Table 1 Selected model parameters

Model Parameters	Value	Units
Maximum time step	1	days
Minimum time step	0.1	days
Monoman Sand hydraulic conductivity	20	m d^{-1}
Coonambidgal Clay hydraulic conductivity	0.1	m d^{-1}
Upper Loxton Sand hydraulic conductivity	10	m d^{-1}
Monoman Sand porosity	0.35	
Coonambidgal Clay porosity	0.6	
Upper Loxton Sand porosity	0.4	
Specific storage Monoman Sand	1.6 x 10^{-4}	

Specific storage Coonambidgal Clay	2.0×10^{-3}	
Specific storage Upper Loxton Sand	1.0×10^{-4}	
Residual water content Monoman Sand	0.04	
Residual water content Coonambidgal Clay	0.04	
Residual water content Upper Loxton Sand	0.04	
Monoman Sand thickness	Up to 12	m
Coonambidgal Clay thickness	Up to 5	m
Upper Loxton Sand thickness	Up to 40	m
van Genuchten alpha for Monoman Sand	1.69	m^{-1}
van Genuchten alpha for Coonambidgal Clay	0.28	m^{-1}
van Genuchten alpha for Upper Loxton Sand	0.8	m^{-1}
van Genuchten beta for Monoman Sand	8.25	
van Genuchten beta for Coonambidgal Clay	2.52	
van Genuchten beta for Upper Loxton Sand	3.6	
Longitudinal dispersivity for Monoman Sand	5	m
Longitudinal dispersivity for Coonambidgal Clay	5	m
Longitudinal dispersivity for Upper Loxton Sand	5	m
Transverse dispersivity for Monoman Sand	0.5	m
Transverse dispersivity for Coonambidgal Clay	0.5	m
Transverse dispersivity for Upper Loxton Sand	0.5	m
Evaporation extinction depth defined by a quadratic decay evaporation distribution function (EDF)	1	m
Evaporation limiting saturation for Eucalyptus & Grass (min)	0.05 & 0.25	
Evaporation limiting saturation for Eucalyptus & Grass (max)	0.9 & 0.9	
Transpiration extinction depth defined by a quadratic decay root distribution function (RDF) for Eucalyptus & Grass	5 & 0.5	m
Leaf area index (LAI) for Eucalyptus & Grass	0.5 & 0.5	$m^2\ m^{-2}$
Tree canopy evaporation for Eucalyptus & Grass	4.5×10^{-4} & 4.0×10^{-4}	m
Transpiration fitting parameter (C1) for Eucalyptus & Grass	0.6 & 0.5	
Transpiration fitting parameter (C2) for Eucalyptus & Grass	0 & 0	
Transpiration fitting parameter (C3) for Eucalyptus & Grass	1 & 1	
Transpiration limiting saturation (wilting point) for Eucalyptus & Grass	0.05 & 0.07	
Transpiration limiting saturation (field capacity) for Eucalyptus & Grass	0.1 & 0.1	
Transpiration limiting saturation (oxic limit) for Eucalyptus & Grass	0.8 & 0.8	
Transpiration limiting saturation (anoxic limit) for Eucalyptus & Grass	0.95 & 0.95	
Rill storage height for river and floodplain	0.001 & 0.01	m
Obstruction storage height for river and floodplain	0 & 0.001	m
Friction (x-plane) for river and floodplain (Manning coefficient)	0.005 & 0.05	$T\ L^{-1/3}$
Friction (y-plane) for river and floodplain (Manning coefficient)	0.005 & 0.05	$T\ L^{-1/3}$
Coupling length for river and floodplain	0.01 & 0.01	m

2.2.4 Boundary conditions

The recorded river level was represented using a time-varying first-type (Dirichlet) condition at the river nodes located at the northern and southern parts of the model boundary (Figure 4). Also, the recorded rainfall and potential evaporation were applied to the surface domain using a time-varying second-type (Neumann) condition. For ET modelling, two types of vegetation were assigned to the floodplain surface nodes including Eucalyptus (deep root depth) and grass (shallow root depth). In the sub-surface (porous media) domain, a constant first type (Dirichlet) boundary condition was specified at the north-eastern part of the domain. A 12 m AHD constant head was adopted from potentiometric contours (AWE, 2013). Zero lateral flux conditions were specified on all other model boundaries which is realistic according to personal discussions with local experts and the Australian Water Environment (AWE) report (AWE, 2013). The two SIS production wells were represented in the model according to the recorded pumping rates and durations and were obtained from Berens et al. (2009) and White et al. (2009). Furthermore, artificial flooding was included in the model using a time-varying first-type (Dirichlet) condition at the floodplain depression for up to 1 m head (12 m AHD). To represent the solute boundary conditions, a first-type (Dirichlet) or constant concentration boundary condition was assigned. Observed groundwater concentrations at the observation wells in the floodplain and river ranged from 300 to 50,000 µS/cm. Hence, constant values were applied at the porous media boundary (representing the regional saline aquifer) and the river nodes.

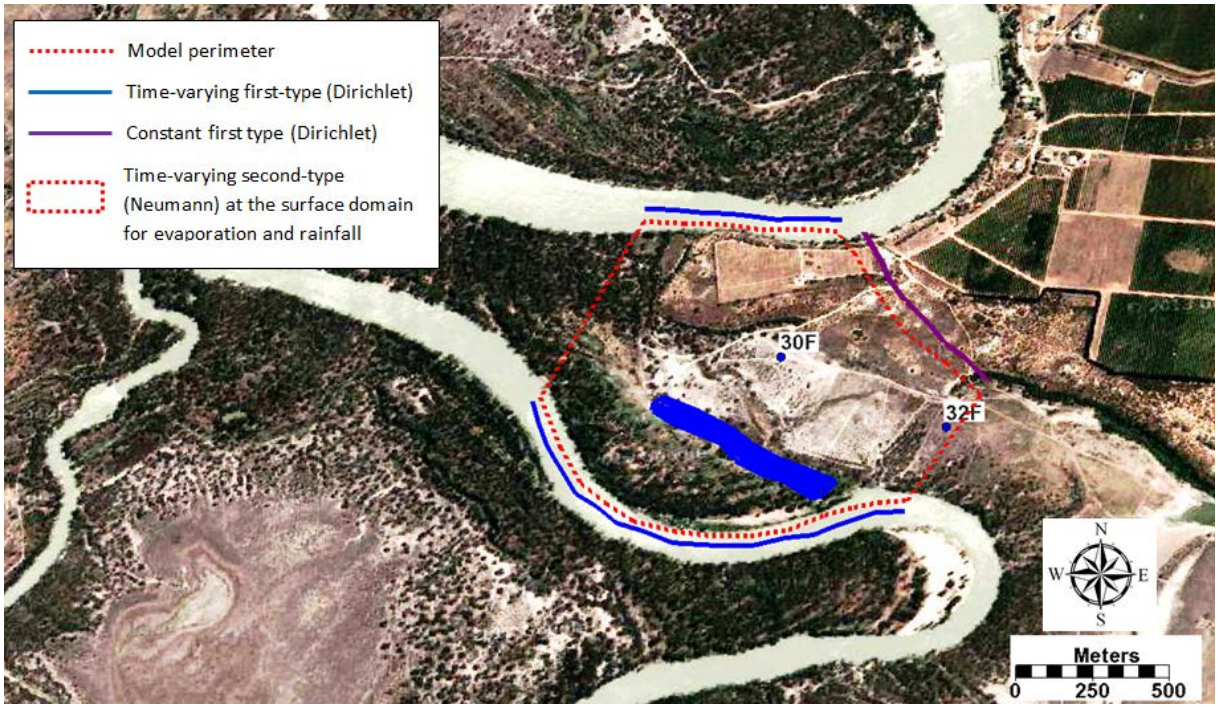
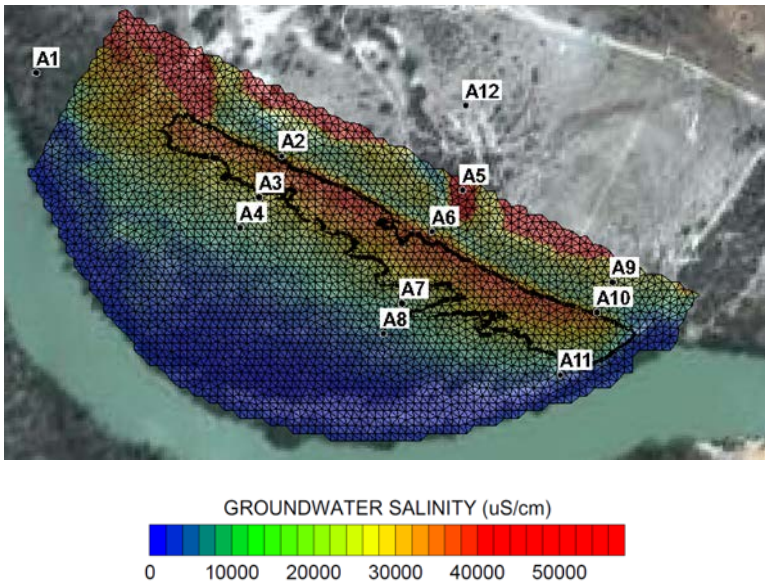


Figure 4. Configuration of the boundary conditions of the model domain

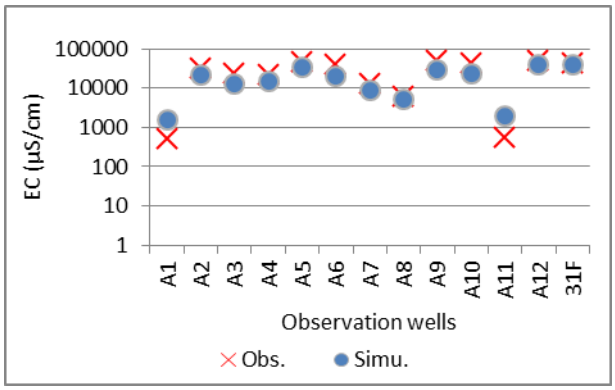
2.2.5 Initial conditions

The initial condition model was generated from a transient simulation of conditions that represented the 50,000 days prior to the first day of the study period (01/07/2005). Outputs from the initial model compared favourably with data from the observation wells on Clark's Floodplain recorded in June 2005 prior to the artificial inundation trials and also EM31 survey in June 2005 before the trials. These were obtained from White et al. (2009).

For instance, Figure 5a shows the simulated pre-trial groundwater salinity distribution which is in a good correlation with EM31 survey in June 2005 (Figure 10b). This is backed up with the results shown in Figure 5b which demonstrates the correlation between the observed and simulated groundwater EC at the location of the 13 observation wells. Considering the observed and simulated results it is apparent that the generated initial condition appropriately represented the status of the river-floodplain system at the beginning of the artificial flooding applications.



a.



b.

Figure 5. a: Simulated pre-trial (June 2005) salinity distribution; b: Correlation between the simulated and observed groundwater salinity in June 2005 at the location of the observation wells.

2.2.6 Scenarios

Four main manipulation scenarios were modelled which differ by management actions. The first of these was a combination of artificial flooding and groundwater lowering (hereafter referred to as "A.Flood+SIS"). In fact, this is the calibration model that showed the observed river-floodplain behaviour during the study period. The second scenario included neither artificial flooding nor groundwater lowering (hereafter referred to as "No manipulation"). The third scenario only included artificial flooding (hereafter referred to as "Only A.Flood"). Finally, the fourth scenario investigated

the impact of groundwater lowering only (hereafter referred to as "Only SIS"). In all cases, natural processes were simulated, including evapotranspiration, the change in river level over time and lateral groundwater flows in and out of the floodplain.

2.2.7 Sensitivity and uncertainty analysis

For a given model, sensitivity analysis identifies whether changes in model inputs lead to large changes in modelled outputs (Yan et al., 2012). The sensitivity analysis involves changing a model parameter by a small amount to establish how model predictions are affected by that change. Manual sensitivity analysis requires changing a single model parameter, re-running the model to obtain a new set of predicted heads and fluxes and observing the effect of the change, either by eye or numerically by differencing (Barnett et al., 2012). In fact, a focus on sensitive parameters can lead to a better understanding and better estimated values and thus reduced uncertainty (Lenhart et al., 2002). Uncertainty analysis is a broader term, encompassing the estimation of uncertainty in model results due to poorly known parameter distributions, observation errors and simplified model assumptions such as omitted processes (Yan et al., 2012).

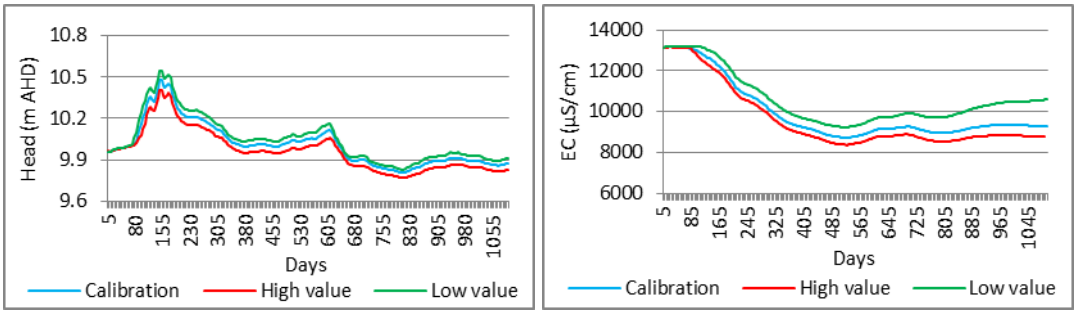
The parameters investigated for the sensitivity analysis are those where there is a degree of uncertainty of their value and where their importance to model results is not immediately clear. Other model inputs are important, but their values are more easily and reliably observed (e.g. SIS pump rates, river levels, rainfall, evaporation and vegetation cover) or are expected to be less heterogeneous and therefore robustly interpolated from observations (e.g. groundwater salinity and potentiometric heads along model boundaries). Also, surface domain parameters are not included in the sensitivity analysis because in the current study all simulations are conducted in non-flooding (non-overbank) conditions and sensitivity of the model outputs to the surface properties are unlikely to be significant.

Table 3 shows the sensitivity analysis parameters and their range of values. The baseline simulation is the calibrated model. In each sensitivity analysis simulation, a single input parameter is changed. The parameter values were varied within a reasonable range around the selected parameter values for calibration. The sensitivity analysis were conducted on a 2D slice along transect 2 (Figure 3c). As the model is calibrated to groundwater head and salinity observations, the sensitivity results are presented in terms of groundwater head and salinity at the location of observation well A7 (Figure 6).

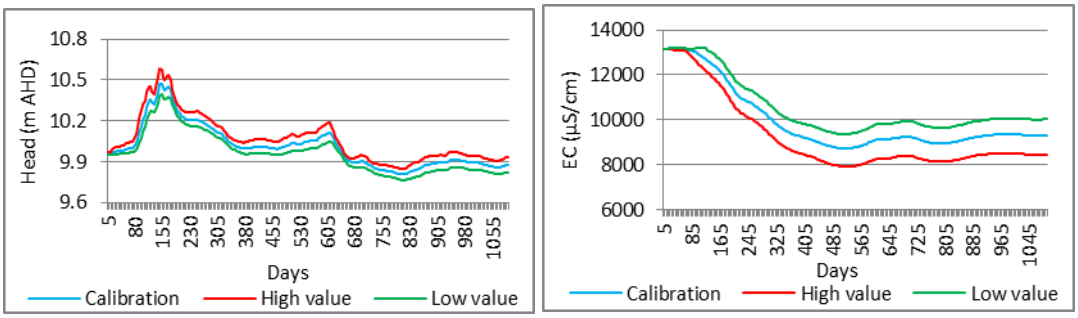
Table 3 Sensitivity analysis parameters and their values

Parameter	Low value	Selected value	High value	Unit
Monoman Sand hydraulic conductivity	15	20	30	m d^{-1}
Coonambidgal Clay hydraulic conductivity	0.05	0.1	0.2	m d^{-1}
Upper Loxton Sand hydraulic conductivity	5	10	15	m d^{-1}
Monoman Sand porosity	0.2	0.35	0.5	
Coonambidgal Clay porosity	0.45	0.6	0.7	
Upper Loxton Sand porosity	0.3	0.4	0.55	
van Genuchten alpha for Monoman Sand	0.8	1.69	3	m^{-1}
van Genuchten alpha for Coonambidgal Clay	0.15	0.28	0.5	m^{-1}
van Genuchten alpha for Upper Loxton Sand	0.4	0.8	1.2	m^{-1}
van Genuchten beta for Monoman Sand	4	8.25	12	

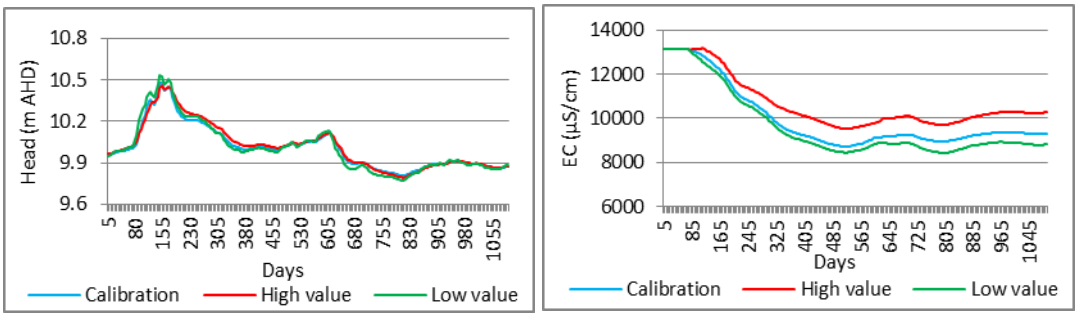
van Genuchten beta for Coonambidgal Clay	1.2	2.52	4	
van Genuchten beta for Upper Loxton Sand	1.8	3.6	5	
Evaporation extinction depth	0.5	1	2	m
Transpiration extinction depth (Eucalyptus)	2.5	5	10	m
Leaf area index	0.25	0.5	1	



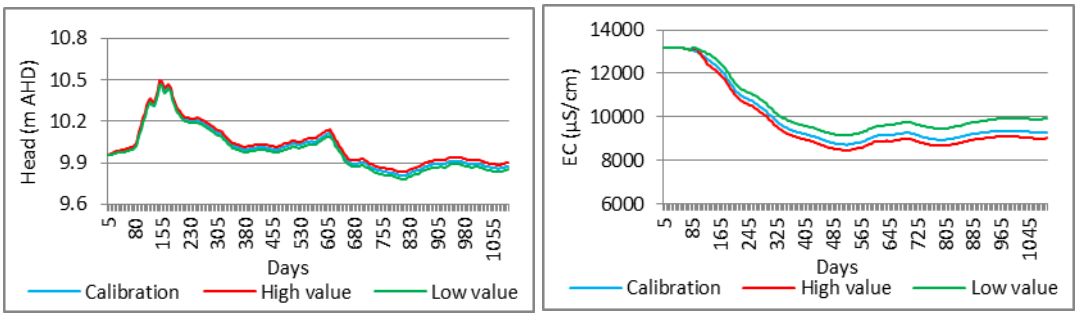
a. Sensitivity of the groundwater head and salinity to Monoman Sand porosity



b. Sensitivity of the groundwater head and salinity to Monoman Sand hydraulic conductivity



c. Sensitivity of the groundwater head and salinity to van Genuchten alpha for Monoman Sand



d. Sensitivity of the groundwater head and salinity to transpiration extinction depth (Eucalyptus)

Figure 6. Results of sensitivity of groundwater head and salinity to the tested parameters

Fifteen properties which are difficult to measure in the field have been used in sensitivity tests and varied within reasonable ranges in the model to determine the impact on model calibration. Among the tested parameters which are listed in Table 3, Monoman Sand hydraulic conductivity and porosity, van Genuchten alpha for Monoman Sand and Transpiration extinction depth (Eucalyptus) show relatively significant impact on the groundwater head and salinity. There are represented in Figure 6. Considering results of the sensitivity analysis of the model, groundwater head is most sensitive to Monoman Sand hydraulic conductivity and porosity. This is because the groundwater flows in the Monoman Sand formation, so, the hydraulic conductivity produces more sensitivity in compare with Coonambidgal Clay or Upper Loxton Sand. However, they show opposite behaviour on the groundwater hydraulic heads. As higher values of Monoman Sand hydraulic conductivity leads to higher groundwater heads. While increase in the porosity creates lower groundwater heads. On the other hand, the groundwater salinity dynamic is significantly sensitive to all the four parameters. In fact, higher values for Monoman Sand hydraulic conductivity and porosity and Transpiration extinction depth (Eucalyptus) may lead to underestimation of the modelled groundwater salinity. While, applying higher value for van Genuchten alpha for Monoman Sand causes over estimation of the modelled groundwater salinity.

3 Results and Discussion

3.1 Model Calibration

In order to calibrate the model, observed data from 12 observation wells were used. The calibration model time frame was from 1/7/2005 to 1/7/2008 (1,095 days). This period covers both the artificial flooding trials that took place in August 2005 and September 2006 as well as the groundwater lowering that took place via the two SIS production wells (30F and 32F). Ideally the model performance measures should include a combination of quantitative and non-quantitative measures (Barnett et al., 2012). The hydraulic conductivity, porosity, dispersivity (longitudinal and transverse), soil formation thickness and leaf area index were adjusted within known ranges and reasonable limits in order to achieve an acceptable match to observed data. For the detailed description on the numerical model calibration reader is referred to Alaghmand et al. (2014b).

In this case, well-documented observed groundwater head data with a reasonable distribution was available. In terms of flow dynamic, the qualitative goodness-of-fit of the calibration was assessed through both visual comparison between the observed and the simulated time series of hydraulic heads and quantitative evaluation using the goodness-of-fit statistics shown in Table 2. For Root Mean Squared Error (RMSE) and Mean Sum of Error (MSE), the ideal values would be zero. Also, the closer the Coefficient of Determination (r^2) and the Nash-Sutcliffe Model Efficiency (NSE) are to 1, the more accurate is the model. Figure 7 presents the simulated and observed groundwater heads at the observations wells along with the recorded river levels. Moreover, ET flux was calculated as 36-222 mm/yr for the study period. This is consistent with Doble et al. (2006) who suggested 40-360 mm/yr for eucalyptus trees and 0-40 mm/yr for grasslands in this area.

Field data can be used to develop and calibrate an accurate salinity map. However, accurate field data with sufficient spatial resolution are often not available (Brunner et al., 2007). Brunner et al. (2007) showed that a combination of field data and remotely sensed data can be used to regionalize point data such as electrical conductivity measured in the field. Here, the combination of the surveyed EM31 data, reported data (Berens et al., 2009; White et al., 2009) and recorded electrical conductivity at the observation wells were used to calibrate the modelled salinity patterns in the floodplain aquifer (See Figures 5a and 102). From Table 2 and Figure 7, it is clear that the calibration model set-up adequately represents the interaction between the river and the floodplain. A detailed description of the evaluation metrics used to assess the numerical model performance is given in Alaghmand et al. (2014b), Bennett et al. (2013), Straatsma et al. (2013), Matthews et al. (2011) and Jakeman et al. (2006).

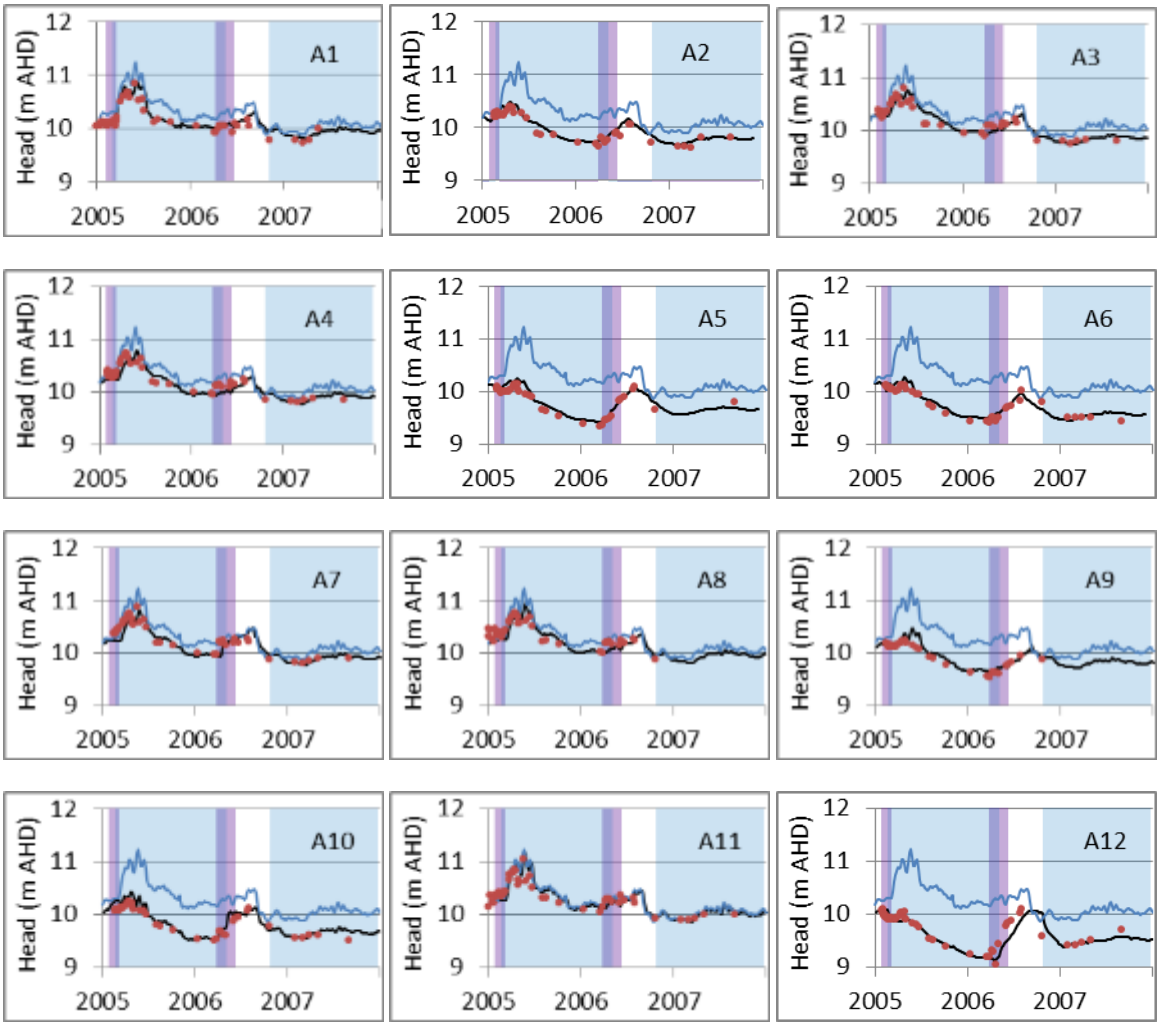


Figure 7. Simulated and observed groundwater heads at the observation wells. River levels and simulated and observed groundwater heads are shown as blue lines, black lines and red dots, respectively. The blue and purple patterns represent the groundwater lowering and artificial flooding, respectively.

Table 2 Model performance evaluation metrics

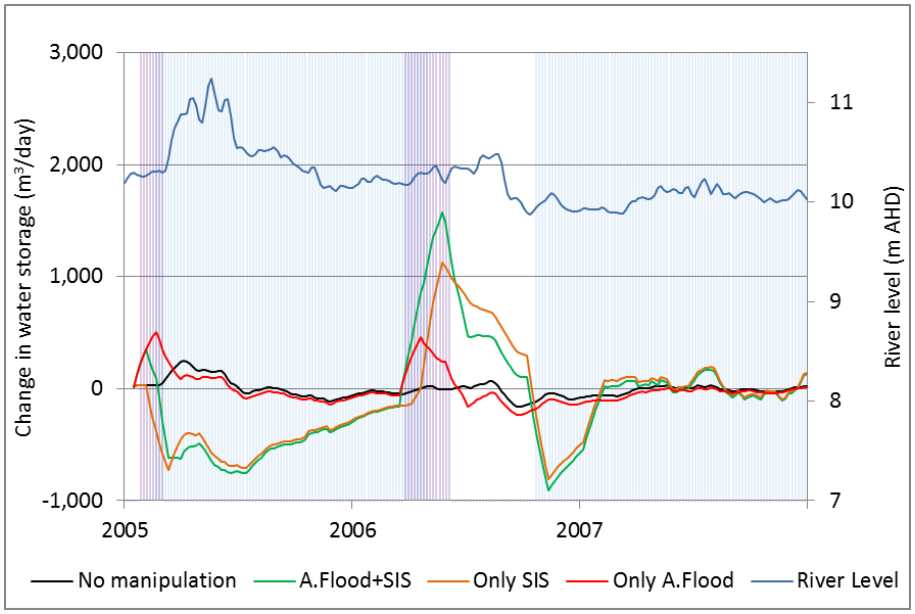
Observation Well	r^2	NSE	MSE (m)	RMSE (m)

A1	0.88	0.84	0.04	0.09
A2	0.87	0.82	0.06	0.09
A3	0.86	0.86	0.07	0.10
A4	0.89	0.85	0.06	0.08
A5	0.82	0.72	0.08	0.11
A6	0.90	0.86	0.80	0.10
A7	0.83	0.81	0.10	0.13
A8	0.75	0.75	0.08	0.12
A9	0.88	0.82	0.07	0.09
A10	0.89	0.85	0.07	0.10
A11	0.94	0.95	0.02	0.05
A12	0.87	0.85	0.04	0.10

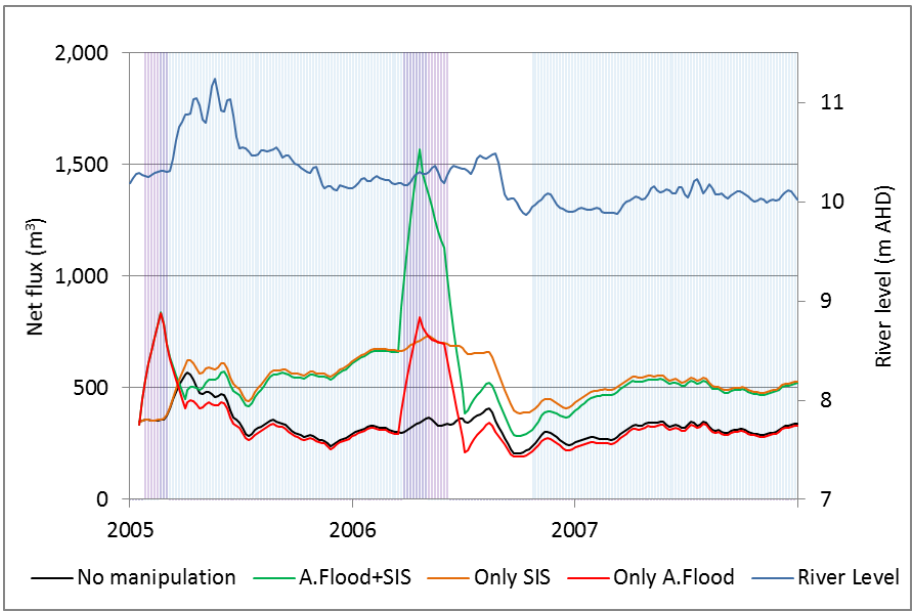
Considering Figure 7, two types of groundwater dynamic regimes in the floodplain can be recognised. The areas relatively close to the river bank are responsive to river fluctuations. This can be noted at observation wells A1, A3, A4, A7, A8 and A11. The response magnitude decreases with distance from the river bank. Hence, those located a long distance from the river banks, such as A2, A5, A6, A9, A10 and A12 are more influenced by the groundwater lowering. Furthermore, artificial flooding does not appear to have a significant impact on the groundwater dynamics of the whole floodplain. Overall, it appears that in this case groundwater lowering has a stronger influence on the floodplain groundwater level dynamic since the artificial flooding and river fluctuation impacts are limited to the inundated area and river bank, respectively.

3.2 Combination of artificial flooding and groundwater lowering

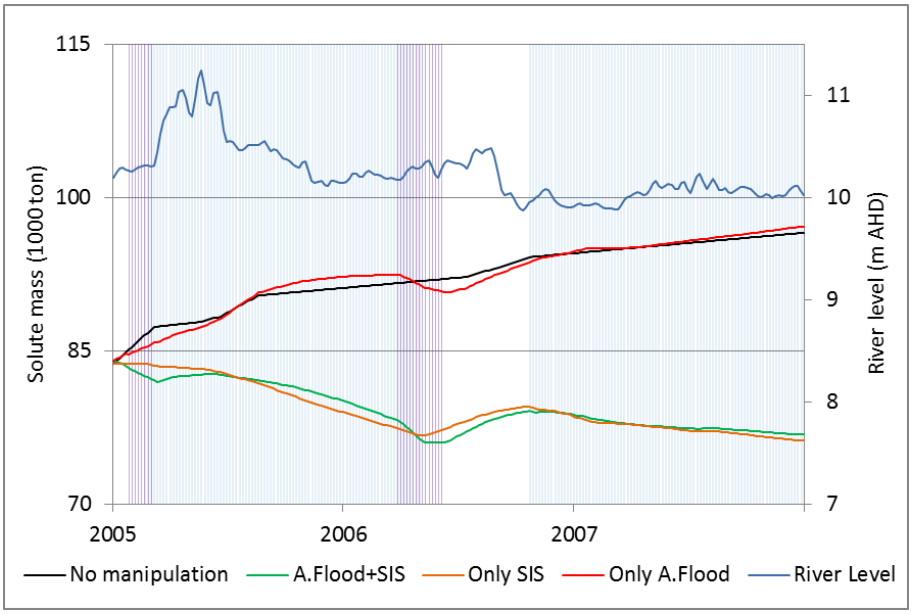
Figure 8a shows the rate of water storage changes (in-out) in each time step in the floodplain aquifer during the study period. The rate value is positive when the recharge rate is more than total discharge rate in each time step and vice versa. Total recharge may include river bank recharges, highland recharge, rainfall and recharge from the inundated floodplain depression. The total discharge refers to the total water removed from the floodplain aquifer via groundwater lowering, ET and discharges to the river and/or highland aquifer.


3,000
2,000
1,000
0
-1,000
Change in water storage (m³/day)
11
10
9
8
7
River level (m AHD)
2005
2006
2007
No manipulation
A.Flood+SIS
Only SIS
Only A.Flood
River Level

a.


2,000
1,500
1,000
500
0
Net flux (m³)
11
10
9
8
7
River level (m AHD)
2005
2006
2007
No manipulation
A.Flood+SIS
Only SIS
Only A.Flood
River Level

b.



c.

Figure 8. a. Change in water storage in the floodplain aquifer. b. Total water flux from the surface domain to the floodplain aquifer. c. Total solute mass stored in the floodplain aquifer. The blue and purple patterns represent the groundwater lowering and artificial flooding, respectively.

Under "No manipulation" scenario, changes in water storage are correlated with river level fluctuations. But, application of groundwater lowering alters this trend. For instance, changes in water storage in the two periods are positive, which can be attributed to the artificial flooding trials. But the second spike in Figure 8a is higher than the first one. To some extent this is due to an increased volume of water pumped to the floodplain depression. But the SIS production wells stopped working mid-way through the second artificial flooding trial due to a fault in the disposal pipeline. Hence, the water accumulation rate in the floodplain aquifer that was increasing during the second artificial flooding trial was accelerated when the groundwater lowering stopped. Therefore, the floodplain aquifer began to recharge from the river and highland aquifer (recharge from rainfall was not plausible) and these added to the recharge from the inundated floodplain depression. On the other hand, it seems that during groundwater lowering the rate at which water leaves the system via the production wells and ET is higher than the floodplain aquifer recharge via the river and inundated floodplain depression. Particularly, at the beginning of the groundwater lowering in August 2005 (after the first artificial flooding trial) and the resuming of this in May 2007, the change in water storage has a high absolute value. Gradually the volume approaches to zero in both of the groundwater lowering periods. This reflects the formation of the pumping drawdown cone. In the second period of groundwater lowering (after resuming in May 2007) the change in water storage reaches zero much quicker compared to the first period (between July 2005 and November 2006). This is because during the second period, groundwater lowering was the main driver, but the first period occurred during a period of high river flow. It appears that the river and floodplain were in an equilibrium condition after August 2007 due to a combination of groundwater lowering and a stable river level.

Figure 8b shows the total water flux from the surface domain (including rainfall, river and artificial flooding) to the floodplain aquifer. Two high river flows occurred during the study period, but neither of these produced a significant impact on the water flux exchange. The first one occurred in just after the first artificial flooding trial. In that period, enhanced groundwater levels beneath the inundated floodplain depression prevented a high rate of water flux from the river. Instead, the floodplain aquifer recharged from the highland aquifer. The second river high flow happened when the production wells were shut down. Consequently, during this period groundwater was rising up and approaching its normal level which led to a decline in the head gradient. This is consistent with the change in water storage in Figure 8a. In fact, the minimum water flux from the river to the floodplain aquifer was calculated in April 2007 when the river level was at its lowest and the production wells were shutdown. This supports the zero change in water storage in Figure 8b.

The water flux exchange between the surface domain and the floodplain aquifer domain suggests that during the artificial flooding and groundwater lowering, the floodplain aquifer recharges from the fresh river water (via river banks/bed and inundated floodplain depression). Hence, a relatively fresher (less saline) floodplain aquifer is expected during those periods. Total solute mass stored in the floodplain aquifer is one of the useful outputs of the model and can be used to investigate the solute dynamic during the study period. Figure 8c shows the simulated total solute mass stored in the floodplain aquifer during the study period for the defined scenarios. It appears during the operation of the salt management measures, relatively less solute mass is accumulated in the floodplain. On the other hand, as discussed earlier and shown in Figure 8b, despite operation of the SIS production wells, a decline in water flux from the surface domain to the floodplain aquifer is observed after the first artificial flooding trial for a short period of time. This implies that the floodplain aquifer is recharged more from the saline highland aquifer than from fresh river water during this period. This is consistent with the slight increase in stored solute mass shown in Figure 8c.

Overall, it appears that application of salt interception measures (including artificial flooding and groundwater lowering) led to a decrease in the amount of stored solute mass in the floodplain aquifer by 4% (Figure 8c). The solute accumulation trend is decreasing except during the period that the SIS production wells were shut down and also after the first artificial flooding trial. In addition, there is no correlation between solute mass accumulation and river level fluctuations when both drivers are in force. Moreover, Figure 8c shows that an absence of salt management measures leads to a 6% increase in the accumulated solute mass in the floodplain aquifer. In this case, the solute mass accumulation does respond slightly to river level fluctuations. As shown in Figure 8c, high river flows lead to a slight decrease in the solute mass accumulation in the “No manipulation” scenario.

3.3 Impacts of artificial flooding

During the artificial flooding the floodplain depression was inundated up to 12 m AHD. This was above the recorded river level at the same time which was around 10.3 m. This led to floodplain aquifer recharge which created a temporary increase in the groundwater level below the inundated floodplain depression. This changed the head gradient towards both the river and the highland sides of the floodplain depression. Consequently, as shown in Figure 9, there might be a potential risk of river salinity risk during the artificial flooding particularly when the groundwater is as saline as the study site. In this case, a maximum groundwater discharge 1500 m^3/day with a salinity in the range of 5,000 and 10,000 mg/L (TDS) produces approximately 15 ton/day of salt during this period (November 2006). During the same period, 4016 ML/day flow was recorded at Lock 4 just upstream of the study site with

a salinity of approximately 200 mg/L (TDS) (WaterConnect, 2013) which would produce approximately 800 ton/day of salt. Hence, in this case, the saline groundwater discharge cannot have more than a 2% impact on the river water quality.

Considering Figure 9, a slight increase in stored solute mass in the floodplain aquifer occurred after both of the artificial flooding trials. This is because the end of the artificial flooding application corresponds to the beginning of the absence of fresh surface water recharge. Consequently, an upward saline groundwater flow appears below and at the edge of the floodplain depression (See Figure 10). Note that even after this slight increase, the groundwater aquifer remained less saline compared with the period before the artificial flooding trials. This is shown in Figure 10 which indicate higher salinities in February 2006 and 2007 at the northern edge of the floodplain depression compared with June 2005 and September 2006, respectively. Depending on the scale of the floodplain and the flooded area, post artificial flooding salinity can be a salinity stress issue for a short period.

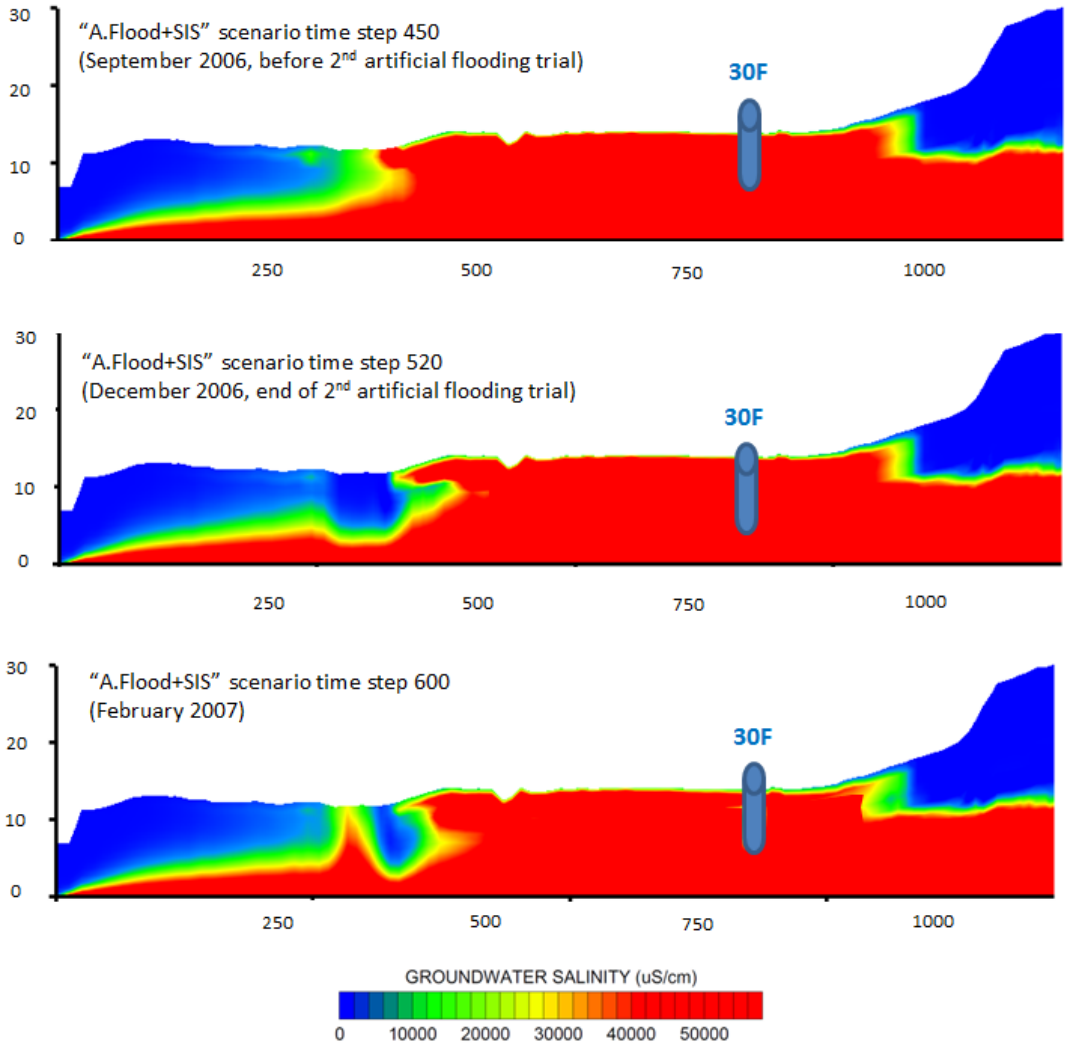


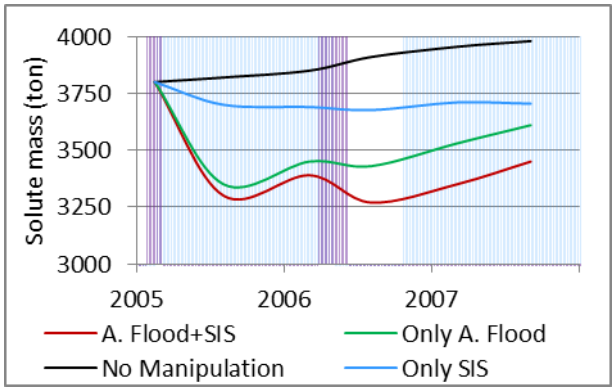
Figure 9. Groundwater salinity along transect 2 at time steps 450, 520 and 600 days (Z magnification: 3).

These results indicate that the impacts of artificial flooding are limited spatially to the inundated areas and temporally to the duration of the trial. For instance, Figure 8c shows that the impacts of

artificial flooding over the whole floodplain are not considerable. Therefore, in order to have a better understanding of the impact of artificial flooding on the solute dynamic of the flooded area, the simulated solute dynamic at the floodplain depression profile has been extracted from the floodplain model. To do this, only nodes located within the boundary of the floodplain depression (yellow line in Figure 2) were chosen and analysed. Hence, a total of 1220 nodes were selected within 37,000 m^2 area of the floodplain depression up to 10 m depth. This is shown in Figure 10a.

It appears that after each of the artificial flooding trials, a significant reduction in stored solute mass may occur. The reduced solute mass during the first trial was only sustained for 4 to 6 months and then increased until the second trial commenced. This correlates with the time taken for the depression to naturally dry evaporation and percolation. Later, after 6 months of the second trial, the solute mass started accumulating in the profile. The general pattern is quite similar for both scenarios but a combination of groundwater lowering and artificial flooding can maintain a relatively less saline profile compared with artificial flooding alone. Despite an increased volume of water applied during the second trial (29.97 ML in the first trial compared to 52.17 ML in the second), it seems that the first trial removed relatively larger amount of solute mass compared with the second trial, perhaps due to less solute mass accumulation between the first and second trials. Furthermore, the salinity after the second trial gradually increased due to a high ET rate and the absence of surface water recharge.

The results of solute dynamic shown in Figures 8c, 9 and 10a can be supported by the EM31 surveys conducted at the study site reported by White et al. (2009) (Figure 10b). The February 2006 survey (Figure 10b) was carried out following dissipation of water from the first flooding trial. Figure 10a shows a noticeable reduction in the bulk conductivity within the extent of the inundation zone. In fact, vertical infiltration of fresh water from the soil surface resulted in a reduction in stored soil chloride at all of the flooded locations. The change is most evident over the eastern half of the inundated area, which is more depressed topographically and is the region where water pools for the longest time. The same pattern is observed after the second trial.



a.

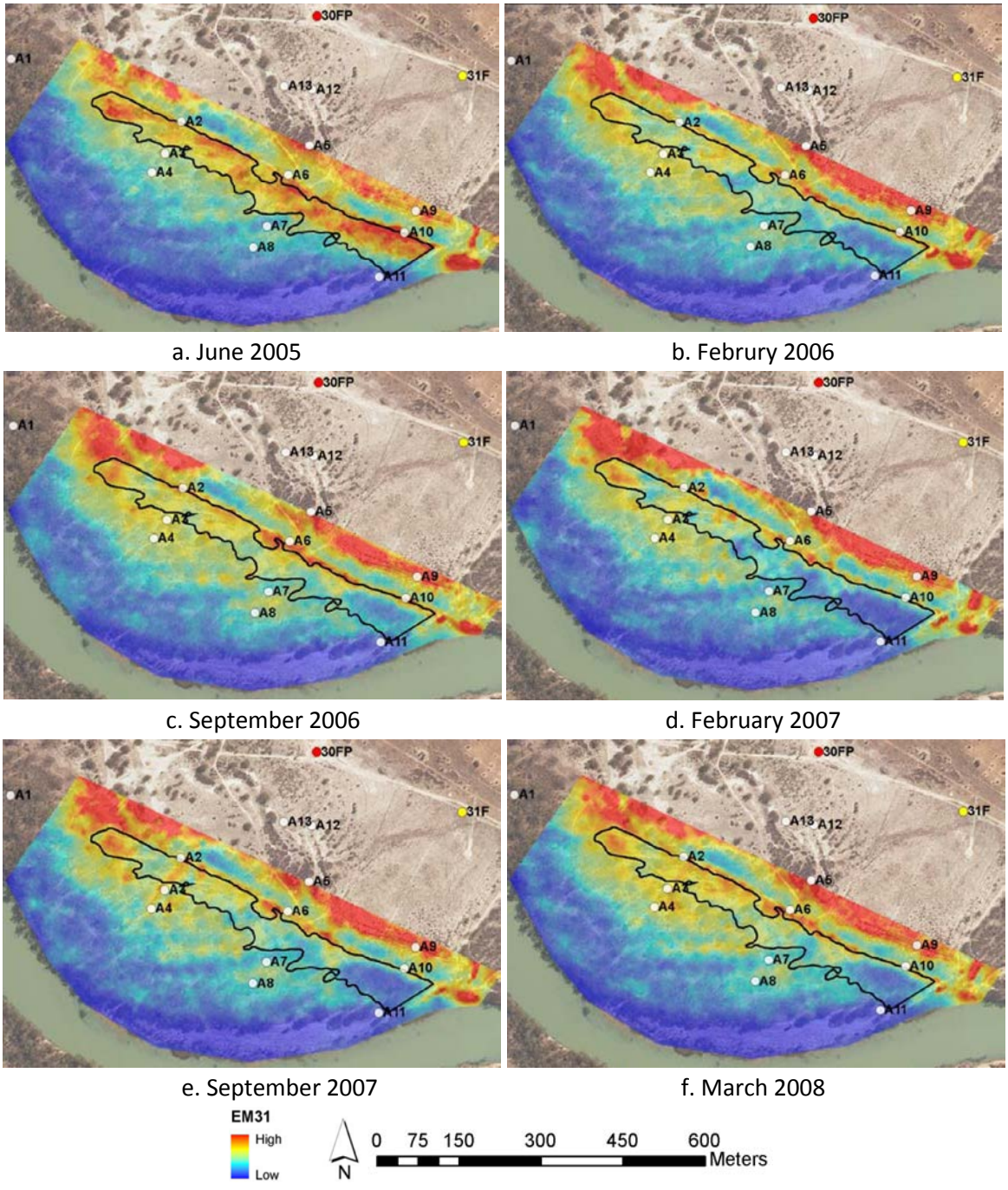


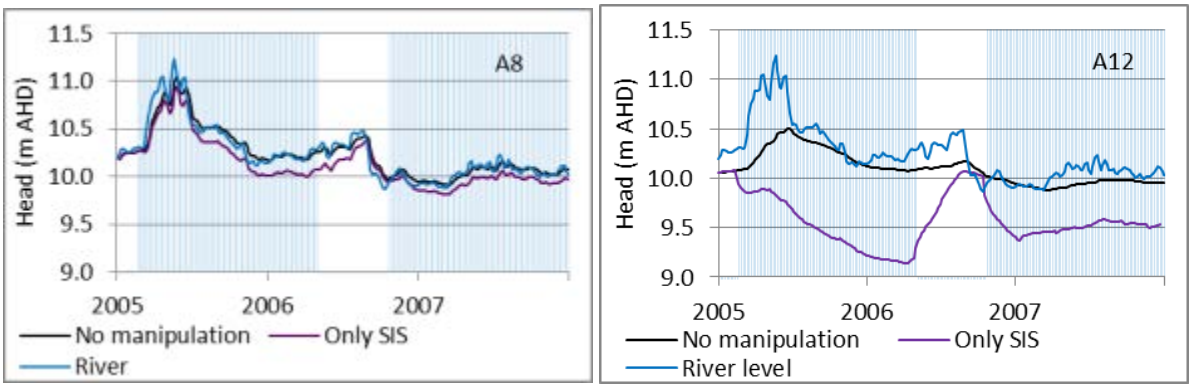
Figure 10. a: Total solute mass stored in the floodplain depression profile for the defined scenarios during the simulated period. The blue and purple patterns represent the groundwater lowering and artificial flooding, respectively. b: Temporal distribution of electrical conductivity using Geonics EM31 at the study site (White et al., 2009)

This study shows that artificial flooding is able to reduce root zone salinity beneath the flooded area and this can lead to improved vegetation health. However, these influences are generally limited spatially to the inundated zone and cannot permanently change the saline nature of the system. The model results are consistent with the findings of White et al. (2009) who investigated vegetation health response to artificial flooding using techniques such as EM31 conductivity surveys, visual tree

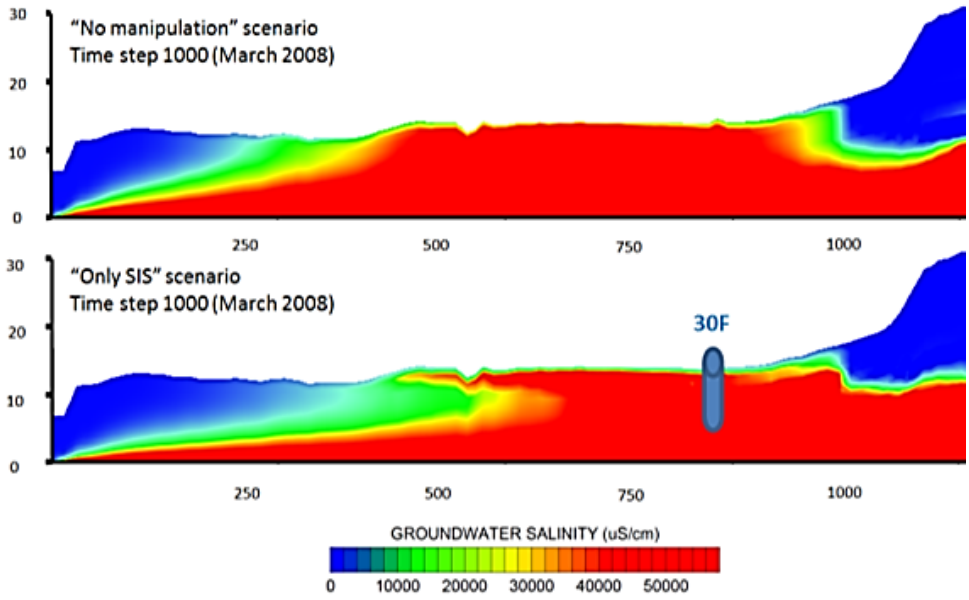
condition assessments, juvenile river red gum heights and understory surveys. White et al. (2009) concluded that physical (water and soil) and biological (vegetation) processes respond favourably to the trials to improve vegetation condition. They recommended that artificial flooding as an intervention technique should be considered when vegetation starts to decline. However, they also found that only trees with crown extents of 25-75% have a high chance of recovering during the intervention period.

3.4 Impacts of groundwater lowering

From Figure 11a, when the production wells are in operation they are able to form a lower floodplain water table. The response of each observation well (or floodplain zone) is proportional to its distance to the production wells and the river. For example, water levels in observation well A8, which is located close to the river bank closely follow the river fluctuations. In contrast, water levels in observation well A12 correspond significantly to the groundwater lowering rates. It seems that when the production wells are shut down, it takes 4 months for the groundwater to return to normal levels. The response of the bores such as A12 near to the production wells is rapid since when the SIS production wells were restarted in May 2007 an immediate drawdown can be observed.



a.



b.

Figure 11. a: River level and simulated groundwater heads at the location of observation wells A8 and A12 for the defined scenarios. The blue pattern represents the groundwater lowering period. b: Groundwater salinity along transect 2 for the "No manipulation" and "Only SIS" scenarios (Z magnification: 3).

In terms of ET flux, the "No manipulation" scenario produces 0.096 mm/day of ET while the "Only SIS" scenario produces 0.088 mm/day. Perhaps this is due to the lowered groundwater table which keeps it below the evaporation depth for longer periods. Moreover, Figures 8a and 8b imply that significant water flux exchange occurs during the operation of the SIS production wells. This is mainly due to the enhanced head gradient towards the floodplain aquifer due to groundwater lowering. For instance, Figure 8b shows that groundwater lowering creates an increased water flux from the surface domain to the floodplain aquifer compared to the "Only A.Flood" and "No manipulation" scenarios. In fact this water flux can be interpreted as river bank recharge (i.e. no rainfall or flood recharge). It appears that when groundwater lowering is in operation it can significantly increase the river bank recharge thereby creating a wider fresh water lens and this maintain a relatively less saline floodplain aquifer.

Figure 11b shows that one side (between the river and the production wells), the groundwater lowering can enhance the fresh water lens due to the boosted hydraulic gradient towards the floodplain aquifer. But on the other side of the production wells (between the production wells and the floodplain highland), the floodplain recharges with saline groundwater from the highland aquifer, which is the source of the solute, making this zone more saline. For example, in this case the average accumulated solute masses on the river and highland sides of the production wells are approximately 7.3 $kg.m^{-3}$ and 17.3 $kg.m^{-3}$, respectively. Therefore, groundwater lowering is only able to keep the solute away from the river but does not completely remove it from the floodplain. In fact, under normal conditions, a gaining river typically recharges from the groundwater aquifer. But, the groundwater lowering (here via SIS production wells) can prevent the occurrence of the saline groundwater recharge by solute mass removal and groundwater level lowering at the same time. It is interesting that the fresh zone at the top right side of Figures 9 and 11b represent the relatively fresh irrigation water from the irrigation practices on the adjacent highland which are consistent with the observed conductivity depth sections across Bookpurnong Floodplain reported by Berens et al. (2009). Therefore, it is clear that attention needs to be paid to the configuration of any groundwater lowering scheme if it is to be an effective measure to prevent saline groundwater discharge to the river and also to obtain a less saline floodplain aquifer. Indeed, if the production wells are located too close to the river banks they may attract more saline groundwater recharge from the highland aquifer and this may lead to a more saline floodplain aquifer. If the aim is to reduce regional groundwater flux into the floodplain, then the wells may be better positioned close to the highland. But, if the aim is to extend the freshwater lens, then the wells may be better located closer to the river, which would benefit riparian vegetation but may be detrimental to the health of vegetation on the highland side of the floodplain.

4 Conclusion

At the Lower River Murray in South Australia, the absence of overbank flooding for almost two decades resulted in severe stress and decline in the condition of long-lived vegetation on the floodplain. Groundwater lowering (via the SIS production wells) was installed to the study site as a salt

interception measure in order to prevent saline groundwater discharge to the river. In addition, two artificial flooding trials have been conducted to improve the floodplain vegetation condition. A three-dimensional fully-integrated physically-based numerical model was developed. To simulate the site during the trials, well-documented observed data were used to calibrate the model. The aim was to explain the interaction between a river and a saline floodplain in a semi-arid area.

According to the model results, groundwater lowering was able to lower the floodplain aquifer water-table and draw low salinity river water into the saline floodplain aquifer. The response of each observation well was proportional with its distance to the production wells and the river. When the production wells are in operation, groundwater lowering is the dominant driver of the river-floodplain interaction. Water storage rates in the floodplain aquifer are driven by both the artificial flooding and groundwater lowering, with positive rates of change during the artificial flooding trials and negative rates during the operation of the SIS production wells. In terms of salinity, it was shown that absence of the salt interception measures would lead to 6% more solute mass stored in the floodplain aquifer. However, a combination of artificial flooding and groundwater lowering resulted in a 4% decrease in accumulated solute mass in the floodplain aquifer. Of these measures, groundwater lowering had the dominant impact on the whole floodplain while artificial flooding was more significant in the localised flood area. It was shown that groundwater lowering maintains a less saline floodplain aquifer by forming a wider fresh water lens on the river side and a more saline zone on the highland side. It was found that installation of the production wells close to the river banks may lead to a wider freshwater lens on the river side and more salt mass accumulation in the rest of the floodplain.

After the artificial flooding has ceased, in the flooded area a slight increase in stored solute mass was observed due to the upward saline groundwater flow that can be formed beneath and at the edge of the floodplain depression. However, it was not able to increase the salinity of the whole floodplain in this case. Saline groundwater discharges to the river occurred during both of the artificial flooding trials. However, the saline groundwater discharges did not have a significant impact on the river water quality in this case, although in smaller river systems with lower flows, this could potentially be an issue. Furthermore, the washed-off solute mass from the soil profile beneath the floodplain depression due to the first artificial flood trial was only sustained for 4 to 6 months and then increased again until the second trial. Overall, it was shown that artificial flooding is an intervention technique that can be considered as a supplement for natural overbank flooding which may decrease the soil and groundwater salinity and improve vegetation health. From an ecological point of view it can be concluded that artificial flooding delivers some of the same benefits as natural overbank floods, with increases in vegetation health condition, restoration of understory seed banks, decreases in soil and groundwater salinity and initiation of river red gum germination. However, its impacts are limited spatially to the flooded area and temporally to the flood duration and therefore artificial flooding cannot completely change the natural condition of the floodplain. Hence, artificial flooding may be considered as a short term management technique and which may need to be applied periodically if it is to be used as an effective for long term strategy.

This management scheme can be implemented in other semi-arid and arid regions for salinity management purpose and also to improve floodplain vegetation health. However, it would depend on availability of the required infrastructures and also feasibility of the application. Therefore, a comprehensive numerical modelling can be useful to quantify impacts of such measures under various scenarios.

5 Acknowledgement

This work was supported by the Goyder Institute for Water Research. The authors would like to acknowledge the assistance and scientific support of Dr. Rebecca Doble (CSIRO), Mr. Volmer Berens (DEWNR), Professor Adrian Werner, Dr. James McCallum (Flinders University) and Dr. Dylan Irvine (Monash University).

6 References

Ala-aho P, Rossi PM, Isokangas E, Kløve B. Fully integrated surface–subsurface flow modelling of groundwater–lake interaction in an esker aquifer: Model verification with stable isotopes and airborne thermal imaging. Journal of Hydrology 2015; 522: 391-406.

Alaghmand S, Beecham S, Hassanli A. Impacts of Groundwater Extraction on Salinization Risk in a Semi-Arid Floodplain. Nat. Hazards Earth Syst. Sci. 2013a; 13: 3405-3418.

Alaghmand S, Beecham S, Hassanli A. A review of the numerical modelling of salt mobilization from groundwater-surface water interactions. Water Resources 2013b; 40: 325-341.

Alaghmand S, Beecham S, Hassanli A. Impacts of Vegetation Cover on Surface-Groundwater Flows and Solute Interactions in a Semi-Arid Saline Floodplain: A Case Study of the Lower Murray River, Australia. Environmental Processes 2014a; 1: 59-71.

Alaghmand S, Beecham S, Jolly ID, Holland KL, Woods JA, Hassanli A. Modelling the impacts of river stage manipulation on a complex river-floodplain system in a semi-arid region. Environmental Modelling & Software 2014b; 59: 109-126.

AWE. Loxton Bookpurnong SIS Atlas. Australian Water Environment, Adelaide, 2013.

Banks EW, Brunner P, Simmons CT. Vegetation controls on variably saturated processes between surface water and groundwater and their impact on the state of connection. Water Resources Research 2011; 47: W11517.

Barnett B, Townley LR, Post V, Evans RE, Hunt RJ, Peeters L, et al. Australian groundwater modelling guidelines. In: report W, editor. National Water Commission, Canberra, 2012.

Bauer P, Held RJ, Zimmermann S, Linn F, Kinzelbach W. Coupled flow and salinity transport modelling in semi-arid environments: The Shashe River Valley, Botswana. Journal of Hydrology 2006; 316: 163-183.

Bennett ND, Croke BFW, Guariso G, Guillaume JHA, Hamilton SH, Jakeman AJ, et al. Characterising performance of environmental models. Environmental Modelling and Software 2013; 40: 1-20.

Berens V, White M, Souter N. Bookpurnong Living Murray Pilot Project: A trial of three floodplain water management techniques to improve vegetation condition. Department of Water, Land and Biodiversity Conservation, Adelaide, 2009.

Beven K. Towards an alternative blueprint for a physically based digitally simulated hydrologic response modelling system. Hydrological Processes 2002; 16: 189-206.

BOM. Bureau of Meteorology (BOM), 2013.

Brookfield AE, Sudicky EA, Park YJ, Conant Jr B. Thermal transport modelling in a fully integrated surface/subsurface framework. Hydrological Processes 2009; 23: 2150-2164.

Brunner P, Cook PG, Simmons CT. Hydrogeologic controls on disconnection between surface water and groundwater. Water Resources Research 2009a; 45: W01422.

Brunner P, Li HT, Kinzelbach W, Li WP. Generating soil electrical conductivity maps at regional level by integrating measurements on the ground and remote sensing data. International Journal of Remote Sensing 2007; 28: 3341-3361.

Brunner P, Li HT, Kinzelbach W, Li WP, Dong XG. Extracting phreatic evaporation from remotely sensed maps of evapotranspiration. Water Resources Research 2008; 44: W08428.

Brunner P, Simmons CT. HydroGeoSphere: A Fully Integrated, Physically Based Hydrological Model. Ground Water 2012; 50: 170-176.

Brunner P, Simmons CT, Cook PG. Spatial and temporal aspects of the transition from connection to disconnection between rivers, lakes and groundwater. Journal of Hydrology 2009b; 376: 159-169.

Brunner P, Simmons CT, Cook PG, Therrien R. Modeling surface water-groundwater interaction with MODFLOW: Some considerations. Ground Water 2010; 48: 174-180.

Busch DE, Smith SD. Mechanisms associated with decline of woody species in riparian ecosystems of the southwestern U.S. Ecological Monographs 1995; 65: 347-370.

Calver A. Riverbed permeabilities: Information from pooled data. Ground Water 2001; 39: 546-553.

DES. Drill Enquiry System. SA Water, Adelaide, 2013.

Doble R, Brunner P, McCallum J, Cook PG. An Analysis of River Bank Slope and Unsaturated Flow Effects on Bank Storage. Ground Water 2012; 50: 77-86.

Doble R, Simmons C, Jolly I, Walker G. Spatial relationships between vegetation cover and irrigation-induced groundwater discharge on a semi-arid floodplain, Australia. Journal of Hydrology 2006; 329: 75-97.

Doody TM, Holland KL, Benyon RG, Jolly ID. Effect of groundwater freshening on riparian vegetation water balance. Hydrological Processes 2009; 23: 3485-3499.

Engeler I, Hendricks Franssen HJ, Müller R, Stauffer F. The importance of coupled modelling of variably saturated groundwater flow-heat transport for assessing river-aquifer interactions. Journal of Hydrology 2011; 397: 295-305.

Freeze RA, Harlan RL. Blueprint for a physically-based, digitally-simulated hydrologic response model. Journal of Hydrology 1969; 9: 237-258.

Furman A. Modeling coupled surface-subsurface flow processes: A review. Vadose Zone Journal 2008; 7: 741-756.

Geng X, Boufadel MC. Numerical modeling of water flow and salt transport in bare saline soil subjected to evaporation. Journal of Hydrology 2015; 524: 427-438.

Guo W, Langevin D. Users guide to SEAWAT: a computer program for simulation of three-dimensional variable-density ground-water-flow. US Geological Survey, Tallahassee, Florida, 2002, pp. 01-434.

Harbaugh AW, M.G. M. User's Documentation for MODFLOW-96, an update to the U.S. Geological Survey Modular Finite-Difference Ground-Water Flow Model. US Geological Survey, Reston, Virginia, 1996.

Hatch CE, Fisher AT, Ruehl CR, Stemler G. Spatial and temporal variations in streambed hydraulic conductivity quantified with time-series thermal methods. Journal of Hydrology 2010; 389: 276-288.

Holland KL, Turnadge CJ, Nicol JM, Gehrig SL, Strawbridge AD. Floodplain response and recovery: comparison between natural and artificial floods. Technical Report Series No. 13/4. Goyder Institute for Water Research, Adelaide, 2013.

Irvine DJ, Brunner P, Franssen HJH, Simmons CT. Heterogeneous or homogeneous? Implications of simplifying heterogeneous streambeds in models of losing streams. Journal of Hydrology 2012; 424-425: 16-23.

Jakeman AJ, Letcher RA, Norton JP. Ten iterative steps in development and evaluation of environmental models. Environmental Modelling and Software 2006; 21: 602-614.

Jarwal SD, Walker, G.R., Jolly, I.D.,. General site description; Salt and Water Movement in the Chowilla Floodplain. In: Walker GR, Jolly, I.D., Jarwal, S.D. , editor. CSIRO Division of Water Resources, 1996, pp. 16-309.

Jolly ID, Walker GR, Thorburn PJ. Salt accumulation in semi-arid floodplain soils with implications for forest health. Journal of Hydrology 1993; 150: 589-614.

Karim F, Kinsey-Henderson A, Wallace J, Arthington AH, Pearson RG. Modelling wetland connectivity during overbank flooding in a tropical floodplain in north Queensland, Australia. Hydrological Processes 2012; 26: 2710-2723.

Kite GW, Droogers P. Comparing evapotranspiration estimates from satellites, hydrological models and field data. Journal of Hydrology 2000; 229: 3-18.

Leblanc M, Tweed S, Van Dijk A, Timbal B. A review of historic and future hydrological changes in the Murray-Darling Basin. Global and Planetary Change 2012; 80-81: 226-246.

Lenhart T, Eckhardt K, Fohrer N, Frede HG. Comparison of two different approaches of sensitivity analysis. Physics and Chemistry of the Earth, Parts A/B/C 2002; 27: 645-654.

Li HT, Brunner P, Kinzelbach W, Li WP, Dong XG. Calibration of a groundwater model using pattern information from remote sensing data. Journal of Hydrology 2009; 377: 120-130.

Liggett JE, Werner AD, Simmons CT. Influence of the first-order exchange coefficient on simulation of coupled surface–subsurface flow. Journal of Hydrology 2012; 414–415: 503-515.

Maheshwari BL, Walker KF, McMahon TA. Effects of regulation on the flow regime of the River Murray, Australia. Regulated Rivers: Research & Management 1995; 10: 15-38.

Matthews KB, Rivington M, Blackstock K, McCrum G, Buchan K, Miller DG. Raising the bar? - The challenges of evaluating the outcomes of environmental modelling and software. Environmental Modelling and Software 2011; 26: 247-257.

McCallum JL, Cook PG, Brunner P, Berhane D. Solute dynamics during bank storage flows and implications for chemical base flow separation. Water Resources Research 2010; 46.

Motta D, Abad JD, Langendoen EJ, García MH. The effects of floodplain soil heterogeneity on meander planform shape. Water Resources Research 2012; 48: W09518.

Munns R. Physiological processes limiting plant growth in saline soils: some dogmas and hypotheses. Plant, Cell & Environment 1993; 16: 15-24.

Naiman RJ, Décamps H. The ecology of interfaces: Riparian zones. Annual Review of Ecology and Systematics 1997; 28: 621-658.

Nouri H, Beecham S, Hassanli AM, Ingleton G. Variability of drainage and solute leaching in heterogeneous urban vegetation environs. Hydrology and Earth System Sciences 2013; 17: 4339-4347.

O'Malley C, Sheldon F. Chowilla floodplain biological study. Nature Conservation Society of South Australia, Adelaide, 1990.

Ohlmeyer RG. Investigation of the feasibility of manipulating water levels in the River Murray. South Australian Engineering and Water Supply Department, Adelaide, 1991, pp. 47.

Rassam DW, Peeters L, Pickett T, Jolly I, Holz L. Accounting for surface-groundwater interactions and their uncertainty in river and groundwater models: A case study in the Namoi River, Australia. Environmental Modelling and Software 2013; 50: 108-119.

Richards LA. Capillary conduction of liquids through porous mediums. Journal of Applied Physics 1931; 1: 318–333.

Roerink GJ, Su Z, Menenti M. S-SEBI: A simple remote sensing algorithm to estimate the surface energy balance. Physics and Chemistry of the Earth, Part B: Hydrology, Oceans and Atmosphere 2000; 25: 147-157.

Russo TA, Fisher AT, Roche JW. Improving riparian wetland conditions based on infiltration and drainage behavior during and after controlled flooding. Journal of Hydrology 2012; 432-433: 98-111.

Slavich PG, Walker GR, Jolly ID, Hatton TJ, Dawes WR. Dynamics of Eucalyptus largiflorens growth and water use in response to modified watertable and flooding regimes on a saline floodplain. Agricultural Water Management 1999; 39: 245-264.

Smerdon BD, Mendoza CA, Devito KJ. Simulations of fully coupled lake-groundwater exchange in a subhumid climate with an integrated hydrologic model. Water Resources Research 2007; 43.

Smith FM, Kenny SK. Floristic vegetation and tree health mapping, River Murray Floodplain, South Australia. Department for Environment and Heritage, Adelaide, 2005.

Smith JWN, Bonell M, Gibert J, McDowell WH, Sudicky EA, Turner JV, et al. Groundwater-surface water interactions, nutrient fluxes and ecological response in river corridors: Translating science into effective environmental management. Hydrological Processes 2008; 22: 151-157.

Sophocleous M. Interactions between groundwater and surface water: The state of the science. Hydrogeology Journal 2002; 10: 52-67.

Straatsma MW, van der Perk M, Schipper AM, de Nooij RJW, Leuven RSEW, Huthoff F, et al. Uncertainty in hydromorphological and ecological modelling of lowland river floodplains resulting from land cover classification errors. Environmental Modelling and Software 2013; 42: 17-29.

Sudicky EA, Jones JP, Park YJ, Brookfield AE, Colautti D. Simulating complex flow and transport dynamics in an integrated surface-subsurface modeling framework. Geosciences Journal 2008; 12: 107-122.

Therrien R, McLaren RG, Sudicky EA, Panday SM. HydroGeoSphere: A Three-Dimensional Numerical Model Describing Fully-Integrated Subsurface and Surface Flow and Solute Transport. Groundwater Simulations Group, University of Waterloo, Waterloo, Canada, 2006.

Therrien R, McLaren RG, Sudicky EA, Panday SM. HydroGeoSphere: A Three-dimensional Numerical Model Describing Fully-integrated Subsurface and Surface Flow and Solute Transport. Code Documentation and User's Guide. Groundwater Simulations Group, University of Waterloo, Waterloo, Canada, 2010.

Timbal B, Arblaster J, Braganza K, Fernandez E, Hendon H, Murphy B, et al. Understanding the anthropogenic nature of the observed rainfall decline across South Eastern Australia. CAWCR technical report; 26, Melbourne, 2010, pp. 202.

Treese S, Meixner T, Hogan JF. Clogging of an effluent dominated semiarid river: A conceptual model of stream-aquifer interactions. Journal of the American Water Resources Association 2009; 45: 1047-1062.

Trigg MA, Cook PG, Brunner P. Groundwater fluxes in a shallow seasonal wetland pond: The effect of bathymetric uncertainty on predicted water and solute balances. Journal of Hydrology 2014; 517: 901-912.

van Genuchten MT. A closed-form equation for predicting the hydraulic conductivity of unsaturated soils. Science Society of America Journal 1980; 44: 892-898.

Verstrepen L. Evaluating rainwater harvesting on watershed level in the semi-arid zone of Chile. Bioscience Engineering. M.Sc. Universiteit Gent, Gent, 2011, pp. 113.

Wang W, Li J, Chen X, Cheng D, Jia J. Estimating streambed parameters for a disconnected river. Hydrological Processes 2014; 28: 3627-3641.

WaterConnect. River Murray Water Data https://www.waterconnect.sa.gov.au/RMWD/Pages/default.aspx, 2013.

White MG, Berens V, Souter NJ. Bookpurnong Living Murray Pilot Project: Artificial inundation of Eucalyptus camaldulensis on a floodplain to improve vegetation condition. Science, Monitoring and Information Division, Department of Water, Land and Biodiversity Conservation, 2009.

Wolman MG, Leopold LB. River floodplains: some observations on their formation. USGS Professional Paper 282-C. US Geological Survey, Washington, 1957.

Yan W, Li C, Woods JA. Waikerie to Morgan Numerical Groundwater Model 2012 Volume 1: Report and Figures. Government of South Australia through Department for Water, Adelaide, 2012, pp. 197.

Zheng C, Wang PP. MT3DMS: A modular three-dimensional multispecies transport model for simulation of advection, dispersion, and chemical reactions of contaminants in groundwater systems; documentation and user's guide. US Army Corps of Engineers, Washington, DC, 1999.

Zilli FL, Paggi AC. Ecological responses to different degrees of hydrologic connectivity: Assessing patterns in the bionomy of benthic chironomids in a large river-floodplain system. Wetlands 2013; 33: 837-845.

Zimmermann S, Bauer P, Held R, Kinzelbach W, Walther JH. Salt transport on islands in the Okavango Delta: Numerical investigations. Advances in Water Resources 2006; 29: 11-29.